

Manuscript Number:

Title: Early-Middle Holocene environmental changes and pre-Neolithic human occupations as recorded in the cavities of Jebel Qara (Dhofar, southern Sultanate of Oman)

Article Type: Green Arabia

Keywords: Holocene; Oman; palaeoenvironment; speleothems; cave sites; land shell accumulations.

Corresponding Author: Dr Remy Crassard,

Corresponding Author's Institution: CNRS

First Author: Mauro Cremaschi

Order of Authors: Mauro Cremaschi; Andrea Zerboni; Vincent Charpentier; Remy Crassard; Ilaria Isola; Eleonora Regattieri; Giovanni Zanchetta

Abstract: Numerous palaeoenvironmental and archaeological studies from southern Arabia (Yemen and Oman) have revealed strong relations between phases of human settlements and climate change linked to the Indian monsoon system. Analyses on speleothems, cave fills, lacustrine deposits and palaeo-mangroves have shown that during the Early to Mid-Holocene, a humid Optimum culminated around 9000-8000 cal yr BP. New results on inland speleothems and cave sediments from the Jebel Qara (southern Oman) are crucial in our depiction of Early and Mid-Holocene climatic evolution and cultural dynamics of the region. These aspects are discussed here, based on new archaeological surveys, excavations, geoarchaeological and micromorphological studies, aiming to better understand connections with Terminal Pleistocene and Early Holocene autochthonous cultures of southern Arabia. Our results suggest that the final Pleistocene was marked by strong aridity, which promoted a widespread thermoclastism within rock shelter and deposition of aeolian sand; on the contrary, the transition towards the Holocene is marked (since c. 12000 cal yr BP) by a progressive increasing in environmental humidity, which permitted the formation of thick strata of peridesert loess. After this phase, the environmental humidity of the Jebel increased and permitted the existence of a large community of land snails; the latter were exploited by Early Holocene hunter-gatherers who lived in the rock shelters between c. 10500-9500 cal yr BP and left consistent accumulations of land shells (escargotières). The maximum of Holocene humidity was reached between 9000-8000 cal yr BP; regional aquifer were recharged and the deposition of calcareous tufa at the entrance of caves started, lasting up to c. 4500 cal yr BP. C and O stable isotopes from calcareous tufa highlights, in accordance with several regional records, the progressive decline of the intensity of the Indian Ocean monsoon and the transition towards arid conditions. In this phase, the area was abandoned and archaeological communities possibly relocated along the coast of central and southern Oman, where they exploited the mangrove environment.

Quaternary International

We the undersigned declare that this manuscript is original, has not been published before and is not currently being considered for publication elsewhere.

We confirm that the manuscript has been read and approved by all named authors and that there are no other persons who satisfied the criteria for authorship but are not listed. We further confirm that the order of authors listed in the manuscript has been approved by all of us.

We understand that the Corresponding Author is the sole contact for the Editorial process. He/she is responsible for communicating with the other authors about progress, submissions of revisions and final approval of proofs.

Signed by all authors as follows:

A handwritten signature in black ink, appearing to be 'Zyland', with a horizontal line underneath the main part of the signature.

CENTRE NATIONAL DE LA RECHERCHE SCIENTIFIQUE

CNRS, UMR 5133, Archéorient
Maison de l'Orient et de la Méditerranée
7 Rue Raulin
69007 Lyon
France

Tel: +33 662 662 646
Email: remy.crassard@mom.fr



13 October, 2014

Re: Quaternary International, *“Early-Middle Holocene environmental changes and pre-Neolithic human occupations as recorded in the cavities of Jebel Qara (Dhofar, southern Sultanate of Oman)”*

Dear Editor:

We report here new results on inland speleothems and cave sediments from the Jebel Qara (southern Oman). They are crucial in our depiction of Early and Mid-Holocene climatic evolution and cultural dynamics of the region. These aspects are discussed here, based on new archaeological surveys, excavations, geoarchaeological and micromorphological studies, aiming to better understand connections with Terminal Pleistocene and Early Holocene autochthonous cultures of southern Arabia. Our results suggest that the final Pleistocene was marked by strong aridity, which promoted a widespread thermoclastism within rock shelter and deposition of aeolian sand; on the contrary, the transition towards the Holocene is marked (since c. 12000 cal yr BP) by a progressive increasing in environmental humidity, which permitted the formation of thick strata of peridesert loess. After this phase, the environmental humidity of the Jebel increased and permitted the existence of a large community of land snails; the latter were exploited by Early Holocene hunter-gatherers who lived in the rock shelters between c. 10500–9500 cal yr BP and left consistent accumulations of land shells (escargotières). The maximum of Holocene humidity was reached between 9000-8000 cal yr BP; regional aquifer were recharged and the deposition of calcareous tufa at the entrance of caves started, lasting up to c. 4500 cal yr BP. C and O stable isotopes from calcareous tufa highlights, in accordance with several regional records, the progressive decline of the intensity of the Indian Ocean monsoon and the transition towards arid conditions. In this phase, the area was abandoned and archaeological communities possibly relocated along the coast of central and southern Oman, where they exploited the mangrove environment.

We believe that this paper will fit with the general themes of the “Green Arabia” special issue of Quaternary International.

On behalf of myself and my co-authors, we thank you in advance for considering this article and look forward to a positive response from you.

Sincerely yours,

Dr. Rémy Crassard
Research Fellow / Chargé de Recherche
Centre National de la Recherche Scientifique, CNRS, UMR-5133 ‘Archéorient’, Lyon, France.

1 **Early-Middle Holocene environmental changes and pre-Neolithic human occupations**
2 **as recorded in the cavities of Jebel Qara (Dhofar, southern Sultanate of Oman)**

3

4 Mauro Cremaschi¹, Andrea Zerboni¹, Vincent Charpentier², Rémy Crassard^{3,*}, Ilaria Isola⁴,
5 Eleonora Regattieri^{5,6}, Giovanni Zanchetta^{4,5,6,7}

6

7 ¹ Università degli Studi di Milano, Dipartimento di Scienze della Terra “A. Desio”, via L.

8 Mangiagalli 34, I-20133 Milan, Italy

9 ² Inrap, UMR 7041 ‘ArScAn’, Maison de l’Archéologie et de l’Ethnologie, Nanterre, France

10 ³ CNRS, UMR 5133 ‘Archéorient’, Maison de l’Orient et de la Méditerranée, Lyon, France

11 ⁴ Istituto Nazionale di Geofisica e Vulcanologia, Via della Faggiola 32, I-56100 Pisa, Italy

12 ⁵ Dipartimento di Scienze della Terra, Università di Pisa, Via S. Maria 53, I-56126 Pisa, Italy

13 ⁶ Istituto di Geoscienze e Georisorse-C.N.R., Via Moruzzi 1, I-56100 Pisa, Italy

14 ⁷ Istituto di Geologia Ambientale e Georisorse-CNR, Area della Ricerca di Roma1 -
15 Montelibretti, Via Salaria Km 29,300, Monterotondo (RM)

16 * Corresponding author: remy.crassard@mom.fr

17

18

19 **Abstract**

20 Numerous palaeoenvironmental and archaeological studies from southern Arabia (Yemen
21 and Oman) have revealed strong relations between phases of human settlements and
22 climate change linked to the Indian monsoon system. Analyses on speleothems, cave fills,
23 lacustrine deposits and palaeo-mangroves have shown that during the Early to Mid-
24 Holocene, a humid Optimum culminated around 9000-8000 cal yr BP. New results on inland
25 speleothems and cave sediments from the Jebel Qara (southern Oman) are crucial in our
26 depiction of Early and Mid-Holocene climatic evolution and cultural dynamics of the region.
27 These aspects are discussed here, based on new archaeological surveys, excavations,
28 geoarchaeological and micromorphological studies, aiming to better understand connections

29 with Terminal Pleistocene and Early Holocene autochthonous cultures of southern Arabia.
30 Our results suggest that the final Pleistocene was marked by strong aridity, which promoted
31 a widespread thermoclastism within rock shelter and deposition of aeolian sand; on the
32 contrary, the transition towards the Holocene is marked (since c. 12000 cal yr BP) by a
33 progressive increasing in environmental humidity, which permitted the formation of thick
34 strata of peridesert loess. After this phase, the environmental humidity of the Jebel increased
35 and permitted the existence of a large community of land snails; the latter were exploited by
36 Early Holocene hunter-gatherers who lived in the rock shelters between c. 10500–9500 cal yr
37 BP and left consistent accumulations of land shells (*escargotières*). The maximum of
38 Holocene humidity was reached between 9000-8000 cal yr BP; regional aquifer were
39 recharged and the deposition of calcareous tufa at the entrance of caves started, lasting up
40 to c. 4500 cal yr BP. C and O stable isotopes from calcareous tufa highlights, in accordance
41 with several regional records, the progressive decline of the intensity of the Indian Ocean
42 monsoon and the transition towards arid conditions. In this phase, the area was abandoned
43 and archaeological communities possibly relocated along the coast of central and southern
44 Oman, where they exploited the mangrove environment.

45

46 **Keywords:** Holocene; Oman; palaeoenvironment; speleothems; cave sites; land shell
47 accumulations.

48

49 **1. Introduction**

50 The Early Holocene climatic (mostly precipitation regime) evolution in southern Arabia is now
51 known thanks to studies of palaeolakes and speleothems in Yemen, Oman, Saudi Arabia
52 and the United Arab Emirates (e.g., Fleitmann et al., 2003; Davies, 2006; Lézine et al., 2007;
53 Parker, 2009). Furthermore, high-resolution oxygen isotope profiles of Holocene stalagmites
54 from several caves in northern and southern Oman and Yemen (Socotra) recently published
55 (Burns et al., 1998; Neff et al., 2001; Fleitmann et al., 2003, 2004, 2007, 2011) provide
56 detailed information on Late Quaternary climatic fluctuations of southern Arabian Peninsula
57 and western Indian Ocean. Palaeoclimatic data were also obtained from sand dunes, loess-
58 like deposits, and paleosols (e.g., Nettleton and Chadwick, 1996; Wilkinson, 1997; Coque-
59 Delhuille and Gentelle, 1998; Preusser et al., 2002; Parker et al., 2006; Pietsch and Kühn,
60 2009; Pietsch et al., 2010).

61 Early Holocene human occupation of south-east Arabian Peninsula is witnessed by
62 lithic assemblages characterized by blade productions and the Fasad points, being
63 considered as a lithic facies that still needs to be clearly defined (Charpentier 2008;
64 Charpentier and Crassard, 2013). The so-called Fasad points are characteristic Early
65 Holocene tanged points made on elongated flakes or blades/bladelets and are rarely found in
66 stratigraphy (e.g., Uerpmann et al., 2013). Nevertheless, they are most often occurring as
67 surface finds, thus making it difficult to understand the relationships between climatic
68 changes and cultural dynamics. The caves and the rock shelters that dot the wadis cutting
69 the southern part of Jebel Qara, a massif facing the coast of Dhofar (southern Oman) provide
70 an important opportunity to fill this gap as they include anthropogenic sediments of the Early
71 Holocene hunter-gatherers occupations interlayered with breccias, loess, and calcareous
72 tufa, which were the products of the local effect of the early Holocene climatic changes.
73 Geoarchaeological research previously performed in the area (Cremaschi and Negrino,
74 2002, 2004) was recently resumed and the results obtained are presented in this paper.

75

76 **2. The study region**

77 The region of Dhofar in south-western Oman, bordering the Hadramawt and Mahra regions
78 of eastern Yemen, is a mountainous and plateau region, with one particular limestone massif
79 (Fig. 1), which separates the coastal plain of Salalah from the Nejd Desert: the Jebel Qara
80 (Cremaschi and Negrino, 2005), representing the continuation in Oman of the Yemeni
81 Hadramawt plateau (Fig. 2). Jebel Qara's top is gently undulating and it reaches the
82 maximum height of ~ 850 m above sea level. From the geological point of view, the massif
83 consists of late Cretaceous to Tertiary limestone (Platel et al., 1992). Geological strata are
84 gently tilted to the North and crossed by systems of faults in the area above the Salalah
85 coastal plain and immediately south of the Nejd Desert. Loess deposits occur along the
86 northern fringe of the jebel and are similar to deposits described on the Yemeni Plateau and
87 dated to the Early Holocene (Nettleton and Chadwick, 1996; Cremaschi and Negrino, 2005).
88 A well developed karst net is present in the Jebel Qara massif and many rock shelters are
89 located along the steep slopes in the southern part of the jebel (Platel, 1992; Hanna and Al-
90 Belushi, 1996); many of them can be interpreted as inland notches (Shtober-Zisu et al., in
91 press). The southern margins of the Jebel Qara are connected to the present-day coastline
92 of the Indian Ocean by an alluvial apron consisting of steep alluvial fans, composed of
93 gravel-dominated sediments and dating mostly to the Upper Pleistocene. At the foot of the
94 fan extensive formations of beach rocks are present together with aeolian sand formations,
95 hanging some meters (up to 3-4 m) above the present day shore, suggesting the position of
96 the sea level at the time of the maximum postglacial rebound (Pirazzoli, 1991). Alluvial fans
97 toward the sea also delimitate several fossil swamp basins, filled by organic matter-rich mud
98 (Platel et al., 1992; Horn and Cremaschi, 2004; Cremaschi and Perego, 2008).

99 Today, southern Oman is a semi-arid land, with annual precipitations ranging from
100 200 to 600 mm; most of them are concentrated between July and September (more than
101 80%), when the monsoonal rain from the Indian Ocean reaches the region (Fleitmann et al.,
102 2004). Jebel Qara forms a barrier against the summer monsoon, which rains support shrubs
103 and trees on the southern coastal side of the mountain; to the North, the plateau gradually
104 becomes an arid steppe (Rogers, 1980; Sale, 1980), where overgrazing have recently

105 enhanced the desertification process and soil loss (Sale, 1980a, 1980b; Rogers,1980). On
106 the contrary, during the Holocene the climate of the region, as of the entire Arabian
107 Peninsula, greatly changed. In fact, high-resolution oxygen isotope curves of Holocene
108 stalagmites from caves in northern and southern Oman and Yemen provided detailed
109 information on climatic fluctuations of southern Arabian Peninsula (Burns et al., 1998;
110 Fleitmann et al., 2003, 2004, 2007, 2011). These variations, controlled by the position of the
111 Intertropical Convergence Zone (ITCZ) and dynamics of the Indian monsoon, are briefly
112 reported: in the Early Holocene rapidly decreasing of $\delta^{18}\text{O}$ values indicates a rapid northward
113 displacement in the latitudinal position of the summer ITCZ and the associated monsoonal
114 rainfall belt; while during the Middle to Late Holocene the summer ITCZ continuously
115 migrated southward and monsoon precipitation decreased gradually in response to
116 decreasing solar insolation (Fleitmann et al., 2004).

117 Dhofar archaeological record for the Early Holocene is mainly characterized by
118 surface sites, but also some very few stratified (e.g., Zarins, 2001, 2013; Hilbert, 2013). The
119 Early Holocene occupations of southern Oman, and more broadly of the whole southern
120 Arabia, are in fact quite unclear, mostly known by blade productions, as well as tanged lithic
121 projectiles (including Fasad points). Very little is known apart these rare typological elements,
122 being even difficult to define the origins and the development of the makers of such
123 industries. While researchers have used different terms to refer to this chronological period
124 such as Late Paleolithic or Epipaleolithic (e.g., Cremaschi and Negrino, 2002; Hilbert, 2013),
125 a consensus has not yet been reached in the scientific community working in this area on
126 how to call this pre-Neolithic period. Discoveries have been too sparse up to now to resolve
127 this debate, the lack of a clear Upper Paleolithic and the exact transition to fully neolithicized
128 societies rendering difficult to do so. The more recent sites dated to the Neolithic period (from
129 c. 8000 cal yr BP) are mostly shell middens along the Omani coasts, with rich and consistent
130 cultural material (e.g., Charpentier, 2008) and frequently linked to mangroves and lagoons
131 (Berger et al., 2005, 2013). The lithic industries are well-known, with specific projectile point

132 types, including trihedral and fluted points that are found in the broader southern Arabian
133 Peninsula (Charpentier, 2004, 2008; Crassard 2009).

134

135 **3. Materials and methods**

136 Beyond deposits related to their recent pastoral use, most of the Jebel Qara's cavities
137 preserve an older sedimentary infilling, which occurred in most of the visited cavities with the
138 same characteristics and consists, from the base to the top, of angular breccia, loess
139 deposits and accumulations of land snails (including charcoal and lithic artefacts), sealed by
140 thick calcareous tufa in form of flowstones (Cremaschi and Negrino, 2005). During the field
141 survey, preliminary test trenches were opened in the cavities KR-213 and GQ-13/23 to
142 investigate the archaeological evidence and to collect samples for micromorphological
143 analysis on the base deposits and geochemical analyses on calcareous tufa. Moreover,
144 charcoal samples were collected and submitted to AMS-¹⁴C radiometric dating; the results of
145 new dating and those reported in Cremaschi and Negrino (2005) are indicated in text and in
146 Tab. 1 as uncal and cal yr BP; calibration is according to the IntCal13 curve (Reimer et al.,
147 2013).

148 Thin sections from undisturbed blocks from the archaeological infilling at the bottom
149 of the Jebel Qara caves (KR-213 and GQ-13/23) have been used to identify the stratigraphic
150 sequence-forming processes and to infer the environmental and anthropogenic factors for
151 sediments accumulation and post-depositional changes (e.g., Courty, 2001; Goldberg and
152 Macphail, 2006; Cremaschi et al., 2014). Oriented and undisturbed blocks from the
153 sediments below the flowstones were collected. Thin sections (5x9 cm) were manufactured
154 after consolidation according to standard methods (Murphy, 1986). Micromorphological
155 observation under plane-polarized light (PPL), cross-polarized light (XPL), and oblique
156 incident light (OIL) of sediment thin sections employed an optical petrographic microscope
157 Olympus BX41 with a digital camera (Olympus E420). For the description and interpretation
158 of thin sections, the reader should consider the terminology and concepts established by

159 Bullock et al. (1985), Stoops (2003) and Stoops et al. (2010). Properties of samples detected
160 by thin section analysis are summarized in Tab. 2.

161 Two different samples were collected from the same flowstone decoration (KR1 and
162 KR3) outcropping from the roof of the KR-213 rock shelter and submitted to geochemical
163 analyses. These samples were cut in the laboratory, put in resin and polished. From polished
164 surfaces, samples for U/Th dating and stable isotope analyses (C and O) were collected.
165 Solid prisms of ca. 200 mg (ca. 3 mm wide along the lamina and 1 mm thick on growth axis)
166 were used (e.g., Regattieri et al., 2014). Eight samples were taken for U/Th dating which was
167 performed at the University of Melbourne (Victoria, Australia), following the method proposed
168 by Hellstrom (2003). Correction for detrital Th content was applied using initial activity ratios
169 of detrital thorium [$^{230}\text{Th}/^{232}\text{Th}$]_i of 1.50 ± 1.50 . Results, indicated as years BP, are summarized
170 in Tab. 3. Samples for stable isotope analyses were drilled using an air drill with a drill bit of 1
171 mm. Average distance between samples of ca. 1.5 mm. Stable oxygen ($\delta^{18}\text{O}$) and carbon
172 ($\delta^{13}\text{C}$) isotope ratios were performed with a Gas Bench II (Thermo Scientific) coupled with an
173 IRMS Delta XP (Finnigan Matt) at the Institute of Geosciences and Earth Resources of CNR
174 in Pisa (Italy). Briefly, carbonate samples of ca. 0.15 mg were dissolved in H_3PO_4 (100%) for
175 one hour at 70°C in sealed vials flushed with helium. The headspace gas (CO_2) is entrained
176 in a helium stream, dried with 2 nafion gas dryer, purified by passing through a gas
177 chromatographic column and then injected in the continuous flow isotope ratio mass
178 spectrometer via an active open split. All the results were reported to the relative Vienna
179 PeeDee Belemnite (VPDB) international standard. Sample results were corrected using the
180 international standard NBS-19 and a set of 3 internal standards: two marbles, MOM and MS,
181 and a carbonatite NEW12, previously calibrated using the international standards NBS-18
182 and NBS-19. Analytical uncertainty for replicated analyses of $\delta^{18}\text{O}$ and $\delta^{13}\text{C}$ were c. 0.15 ‰.

183

184 **4. Results**

185 **4.1. Description of the cave infillings and micromorphology of the deposits**

186 The entrance and the outer part of karst cavities and rock shelters, which are exposed at
187 different heights along the slopes of the wadis of Jebel Qara, are systematically covered by
188 calcareous tufa in shape of large flowstones, stalactites and stalagmites. Calcareous tufa
189 accretion is today inactive and they are on the way to collapse and being dismantled;
190 therefore, they are evidence of former higher precipitation in the area (Cremaschi and
191 Negrino, 2005). The calcareous tufa flows cover and preserve a complex stratigraphic
192 sequence composed from the base of angular breccia, aeolian dust and accumulations of
193 land snails, which are associated to anthropogenic deposits. Land snails and associated
194 evidence of human activity (lithic industries and charcoal) have been found only inside the
195 rock shelters and caves opening along the valley bottom, while they lack inside the cavities
196 located to higher elevation along the slope of the wadis. In the latter type of rock shelter
197 calcareous tufa lies directly on angular breccia and aeolian dust. The rock shelters here
198 discussed, site KR-213 and GQ-13/23, are located along the Wadi Jenikermat and may be
199 considered as the reference sequences for the region (Fig. 3).

200 The infilling of site KR-213 consists, from the bottom to the top of the sequence, of
201 three main sedimentary Units (Figs. 3, 4), A to C, sealed by a thick layer of calcareous tufa,
202 Unit D (Cremaschi and Negrino, 2005). The lowermost Unit (A) is a clast-supported angular
203 breccia, associated with intergranular sand. The breccia, derived from the fragmentation of
204 the rock shelter vault, is composed of coarse and medium clasts organized in irregular,
205 discontinuous, non-parallel planar layers that dip towards the mouth of the cave and have an
206 abrupt contact with the underlying bedrock. The intergranular fine fraction is composed of
207 rounded and sub-rounded sand-sized quartz, feldspar, and other mineral grains, interpreted
208 as an aeolian input to sedimentation. The overlying Unit B is a matrix-supported breccia,
209 consisting of very few medium-sized angular fragments of limestone interbedded with brown
210 massive loam. Few thin (about 2 cm), discontinuous, dark brown archaeological layers, all
211 rich in charcoal and flint artefacts, have been identified within this Unit. Cremaschi and
212 Negrino (2005) have demonstrated that the fine fraction has a loess-like grain-size
213 distribution, suggesting input of aeolian silt. A charcoal chunk from the upper part of this Unit

214 permitted to date it at 9130 ± 290 uncal yr BP (11092–9551 cal yr BP). The following Unit C
215 consists of a high concentration of land snails dispersed in a silty matrix, often showing a
216 clast-supported pattern; shells are arranged in discontinuous, nonparallel planar layers
217 several centimetres thick. Unit B has been radiocarbon dated to 8720 ± 60 uncal yr BP (9903–
218 9547 cal yr BP). The mollusc assemblage mostly includes *Euryptyxis latireflexa* and *Revoilia*
219 *dhofarensis*, generally complete specimens in some cases broken and distributed on planar
220 layers (Cremaschi and Negrino, 2005); these species are representative of mesophilous
221 species, adapted to a dense grass cover and requiring wet conditions and vegetal cover
222 (Wright, 1963; Wright and Brown, 1980). Finally, the uppermost Unit A is a thick flowstone
223 deposits sealed with stalagmites, descending from the roof of the shelter and covering the
224 sedimentary fill. The calcium carbonate that formed the flowstones also deeply penetrated in
225 the underlying stratigraphic sequence and most of the layers are moderately to strongly
226 cemented.

227 The sedimentary infilling of cave GQ-13/23, discovered during the field season 2013
228 along the same wadi a few kilometres downstream of the KR-213 shelter, displays a rather
229 similar stratigraphic sequence (Fig. 4). Unit A is not represented in the section investigated,
230 while the Unit B, occurring at the base of the sequence, consists of thin and discontinuous
231 layers of clast- to matrix-supported breccia. Unit C is a particularly thick (~ 1 m) and strongly
232 cemented layers, constituted of gently deepening silty layers including a high concentration
233 of land snails. It is interesting to notice that Unit B at site GQ-13/23 is intercalated with silty
234 layers very rich in angular fragments of charcoal and flint artefacts including a well preserved
235 Fasad point (Fig. 5). A sample of charcoal from the Unit B has been dated to 10040 ± 50 uncal
236 yr BP (11798–11311 cal yr BP). Two radiocarbon dates were obtained on charcoal
237 fragments collected at different levels of the Unit C (Tab. 1), giving 9150 ± 50 uncal yr BP
238 (Unit B; 10486–10226 cal yr BP) and 9010 uncal yr BP (Unit C; 10250–9934 cal yr BP). Also
239 in the case of site GQ-13/23, a thick flowstone descending from the roof of the shelters (Unit
240 D) seals the whole stratigraphic sequence.

241 Interesting information can be detected at the micro-scale; thin sections from the
242 infilling of both caves display similar features (Tab. 2). Thin sections of the clast-supported
243 breccia Units A and B highlight the presence of limestone angular clasts (breccia), probably
244 deriving from thermal degradation of the vault of the rock shelter. In and intergranular
245 position with respect of the limestone clasts sand grains (Unit A) and loess-like (Unit B)
246 sandy silt (increasing in percentage from Unit A to Unit B) occur. The local origin of limestone
247 clasts is confirmed by the occurrence of marine microfossils typical of the rock formations
248 constituting the Jebel Qara (Fig. 6). On the contrary the intergranular sediments, as rich in
249 quartz, feldspar and heavy minerals (Cremaschi and Negrino, 2005), are unrelated to the
250 local geological context and were originated from the deflation of the sands of the Nejd
251 desert. At the microscopic scale, the overlying Unit C includes a high concentration of large
252 fragments of land snails, in some cases broken and distributed in planar layers (Fig. 7). The
253 occurrence of loess sediments as in this unit indicates that the dust supply from the Nejd
254 desert was still active, but the occurrence of pedorelicts due to colluvial processes indicates
255 wetter environmental conditions in comparison with those that drove the formation of the
256 underlying deposit.

257

258 **4.2. Flowstone chronology and geochemical analyses**

259 A total of eight U-series dating have been performed on two samples KR1 and KR3 collected
260 from the same flow stone decoration sealing the base deposits of the KR-213 shelter.
261 Unfortunately, due to the low U content and high level of detrital (Th) contamination, only the
262 result of five out eight ages can be considered as reliable (Tab. 3). U/Th ages indicate that
263 flowstone KR1 is basically older than KR3 (Tab. 3 and Fig. 8); KR1 formed in the Early
264 Holocene between c. 9500 and 7500 yr BP, whereas KR3 precipitated in the Middle
265 Holocene between 5500 and 4500 yr BP.

266 Despite this, stable isotopes from both samples show some similarities, which are
267 particularly strong in the top sections, where isotopes (both oxygen and carbon) show
268 significant excursion toward higher values (Figs. 8 and 9). Carbon values range between -12

269 and -3 and oxygen values are between -2 and 1. Kinetic fractionation sometimes occurs in
270 cave-entrance speleothems and calcareous tufa (Mickler et al., 2006), but in the present
271 case (Fig. 9) carbon isotopic composition shows a low positive correlation with oxygen record
272 ($R^2=0.52$ for KR1 and $R^2=0.2$ for KR3). In sample KR3 at ~20 mm from the top, there is a
273 sharp change in texture and fabric, marked by a thin whitish layer, suggesting the possibility
274 of a hiatus. Because this interval is not chronologically constrained, it would correspond to
275 the top of sample KR1. Owing to this uncertainty the upper interval of KR3 at this stage was
276 not further considered. A simple, linear age model was then constructed for both samples;
277 the ages model need considered as largely indicative (Fig. 8).

278

279 **4.3 Archaeological content of the deposits**

280 At GQ-13/23, as previously observed in neighbouring sites and in those located along Wadi
281 Darbat (Cremaschi and Negrino, 2002, 2005), the Fasad points are present, attesting a
282 human occupation by hunter-gatherers during the Early Holocene. One point in particular
283 (Fig. 5), which has been collected *in situ* (in Unit C, dated to 10486-10226 yr cal BP), is
284 made on a pointed blade showing a bi-lateral convergent preparation with the removal of two
285 previous blades creating a Y-shape guiding arises in order to obtain a final pointed blade.
286 This method of blade production reminds the (probably) contemporaneous methods
287 observed in inland Dhofar sites (Hilbert, 2014) or in Hadramawt, Yemen (Crassard, 2008).
288 The Fasad point from GQ-13/23 is 62 mm long with an abrupt-retouched tang along about
289 one quarter of the piece total length, being typologically much closed to the specimens found
290 in the vicinities (Cremaschi and Negrino, 2002). More broadly, it has many typological
291 resemblances with other examples known from surface sites in Dhofar and elsewhere in
292 Oman and the United Arab Emirates (Charpentier and Crassard, 2013). Very few lithics have
293 been found in relation to this point at GQ-13/23, making difficult to propose a precise
294 technological assessment of the complete lithic assemblage. Nevertheless, both type and
295 technology observed on this single artefact at GQ-13/23, confirm the chronological and thus
296 cultural affiliation of this industry to the Early Holocene. However, it is not firmly known, still

297 highly debated, if the makers of this kind of projectiles have a local origin related to
298 autochthonous Late Paleolithic groups. As well, it is not known if the occupants at GQ-13/23,
299 and their counterparts in the region who were making these Fasad points, are actually the
300 direct ancestors of the Neolithic populations that rapidly spread inland and along the coasts
301 about two millennia later. Only a complete stratigraphic sequence yielding remains of
302 occupations from the Terminal Pleistocene up to the Neolithic period would help in answering
303 such a crucial archaeological issue .

304

305 **5. Discussion**

306 **5.1. Evolution of the climate during the Early and Middle Holocene**

307 The four different units described in the rock shelters of Jebel Qara permit to trace the Late
308 Quaternary environmental evolution of the massif. The whole sequence ranges from c.
309 11798–11311 cal yr BP (calibrated ^{14}C age) to c. 4230 yr BP (U/Th age), including the whole
310 Early and Middle Holocene.

311 The sedimentary processes leading to the formation of the clast- to matrix-supported
312 breccia at the bottom of the stratigraphic sequences appear to be related to thermoclastic
313 shattering of the rocky walls of the cave (Cremaschi and Negrino, 2005) and has to be
314 related to arid climatic conditions. Aeolian sand and silt included in the fine fraction indicate
315 dust transport by strong northerly winds from the Nejd desert. This phase can be dated to a
316 Late Pleistocene/very Early Holocene dry phase (Sanlaville, 1992; Fleitmann et al., 2004). In
317 the Unit B, the breccia decreases or completely disappears and the loess fraction becomes
318 dominant and may be correlated with the peridesert loess deposits of the same age
319 occurring at the northern fringe of Jebel Qara (Cremaschi and Negrino, 2005), and suggests
320 a phase in which northerly winds are still important. The deposition of peridesert loess in
321 southern Arabian Peninsula was put in relation to slightly humid environmental conditions,
322 allowing the growth of vegetation (herbs and bushes) able to trap dust particles (Pye, 1987,
323 1995; Coudé Gausson, 1991; Wright, 2001). Therefore, the transition between Units A to B

324 occurred under progressively more humid environmental conditions, presumably triggered by
325 the resumption of the Indian Ocean monsoon system and the northward shift of the ITCZ.

326 The Unit C is mainly characterized by a large content of shells of mesophilous land
327 snails, indicating the spreading of a savannah-like environment; the sedimentation of this
328 Unit has been interpreted (Cremaschi and Negrino, 2005) as a consequence of the onset of
329 wetter conditions in comparison to that of the underlying loess and breccia deposits. While
330 the ecology of the molluscs supports a climatic interpretation, their occurrence in high
331 concentration inside the rock shelters has to be interpreted as due to human activity as it will
332 be discussed in detail in the next section.

333 An outstanding increase in precipitations intensity is indicated by calcareous tufa,
334 which constitutes the Unit D. Their formation was triggered by the progressive reinforcement
335 of the Indian Ocean monsoon system and the northward shift of the ITCZ, which contrasted
336 the northern winds responsible of sand and loess transport recorded in the underlying units.
337 The stratigraphic sections of the Jebel Qara recorded the progressive increasing in the
338 intensity of precipitations toward the uppermost Unit D of calcareous tufa. In fact, the
339 deposition of freshwater carbonates in arid lands requires a major shift in geomorphologic
340 processes and in climate (e.g., Smith et al., 2004; Cremaschi et al., 2010). Calcareous tufa at
341 Jebel Qara formed since the beginning of the wet Holocene at c. 9000 yr BP (U-series age)
342 and survived up to the start of its decline, at the beginning of the late Holocene arid phase
343 (Hoorn and Cremaschi, 2004).

344 The investigation on the speleothems collected from Unit D offers a more detailed
345 palaeoenvironmental reconstruction. In fact, even though they are generally less laminated
346 and pure than speleothems, cave-entrance calcareous tufa may represent a powerful tool for
347 palaeoenvironmental reconstruction in arid lands (e.g., Smith et al., 2004; Moeyersons et al.,
348 2006; O'Brien et al., 2004; Cremaschi et al., 2010). Following the interpretation reported for
349 speleothem of the area, lower oxygen isotope values indicate higher humidity related
350 (amount effect) to northward displacement of Indian monsoon domain, which occurred at
351 time of higher summer insolation in the northern Hemisphere (Burns et al., 1998; Fleitmann

352 et al., 2003, 2004, 2007, 2011). On the contrary, higher oxygen isotope values are connected
353 to phases of reduced precipitation associated to weakening of the monsoon system and
354 increasing importance of northern, drier winds. The composite record of samples KR1 and
355 KR3 is (up to now) too discontinuous for inferring detailed short term oscillation, but we note
356 that the most negative $\delta^{18}\text{O}$ values were reached at the beginning of the Holocene,
357 suggesting the maximum of precipitation. This was followed by a progressive increase of
358 $\delta^{18}\text{O}$ values, interpreted as a decline in the intensity of the monsoon system. Carbon isotopic
359 compositions show a low positive correlation with oxygen record (Fig. 9); correlation between
360 C and O is often interpreted as indicative of kinetic fractionation (Mickler et al., 2006), this
361 can be also driven by climatic effect (Drysdale et al., 2004; Cremaschi et al., 2010). In
362 particular, during drier period reduction in soil development can produce effect like
363 decreasing in soils productivity and decreasing recharge promoting, for instance prior calcite
364 precipitation (e.g., Genty et al., 2003; Drysdale et al., 2006). These processes can produce
365 increasing of carbon isotopic composition along with higher oxygen isotope values due to the
366 decreasing in monsoon strength. The apparent significant increasing in both oxygen and
367 carbon isotope composition at the top of both samples may indicate the progressive
368 obsolescence of the flow preannouncing the end of calcite deposition, which would have
369 been occurred for the definitive reduction in water recharge due to climate condition.

370 In our case study, an independent control on acquired data is offered by the
371 comparison (Fig. 10) with many curves from Holocene speleothem of Oman discussed by
372 Burns et al. (1998) and Fleitmann et al. (2003, 2004, 2007, 2011). The range of oxygen
373 isotope values measured in our flowstones partially overlaps the values measured in cave
374 speleothems from northern and southern Oman (Fleitmann et al., 2004, 2007). Arguably, this
375 is a good indication of the potential of these flowstones to preserve important hydrological
376 information despite their high superficiality, which often can promote isotopic kinetic
377 fractionation. Moreover, the composite record of samples KR1 and KR3 is evidently similar to
378 Fleitmann's record from Q5 speleothems is quite evident (Fig. 10). Notably, the $\delta^{18}\text{O}$ record
379 of sample KR3 is basically lower than the KR1, in agreement with the general trend of

380 speleothems from site Q5. Finally, in sample KR1 the end of deposition can be roughly
381 constrained at ca. 7.5 ka BP, when Q5 speleothem show a clear monotonic increasing of
382 $\delta^{18}\text{O}$ values.

383 At the regional scale, in the Early and Middle Holocene the southern Arabia
384 experienced a generalized increasing of environmental humidity (e.g., Lézine et al., 1998;
385 Neff et al., 2001; Fleitmann et al., 2004; Parker et al., 2004), triggered by the intensification
386 of the monsoonal precipitation as a consequence of an enhanced solar heating across the
387 northern Hemisphere (Berger and Loutre, 1991; Sirocko et al., 1993; Gasse and Van Campo,
388 1994). This span has been identified as a major phase of permanent lacustrine environment
389 in the Rub' al-Khali sand sea and in the arid regions of Yemen (e.g., McClure, 1976; Schulz
390 and Whitney, 1986; Parker et al., 2004, 2009; Lézine et al., 2007).

391 Finally, it is interesting to take into account the work of Lézine et al. (2007) on the
392 response of a freshwater environment of the Ramlat as-Sabatayn sand sea in continental
393 Yemen to the increase of the Indian monsoon strength. Their archive shows a maximum of
394 Holocene water availability at c. 9000-8000 cal yr BP, as in the whole region; but it also
395 highlights some differences respect to the highly detailed record of precipitation of
396 speleothems (Fleitmann et al., 2003). At Ramlat as-Sabatayn the initial increase of monsoon
397 precipitation is dated from c. 12000 cal yr BP, whereas due to the necessity to the recharge
398 of the mountain aquifers the sedimentation of speleothems started later. In the Jebel Qara
399 this phase corresponded to the beginning of loess sedimentation and therefore, according to
400 our interpretation, to the initial spread of vegetation able to trap dust particle as consequence
401 of enhanced precipitation. This possibly confirms that the strengthening of the Indian Ocean
402 monsoon started at the very beginning of the Holocene.

403

404 **5.2. Early Holocene human occupation of the cavities Jebel Qara**

405 Evidence of human occupation (lithic industry and charcoal) in the cavities of Jebel Qara is
406 mostly concentrated in the Unit C, a part of the occasional find of charcoal in Unit B, and it is
407 systematically associated with high concentration of mollusc shells. At the macroscopic

408 scale, molluscs and archaeological evidence occur only in the cavities located in the valley
409 floors of easy accessibility. On the contrary in the caves and shelters, hanging at different
410 heights along the steep valley slopes, molluscs and artefacts are absent and calcareous tufa
411 directly overly Units A and B. Inside the cave deposits molluscs are associated to organic
412 layers, charcoal, in some case to small fragments of burned bones and to lithic artefacts. In
413 thin section, the evidence of human activity is clearer as shells of land snail are often broken
414 and redistribute in flat layers with planar distribution of clasts and associated to finely
415 subdivided organic matter and charcoal lenses; these are indicative for occupational
416 trampling (e.g., Gé et al., 1993; Zerboni, 2011). Moreover, the micromorphological
417 investigation of the mollusc rich strata showed, in some cases, evidence for heating of shells,
418 represented by peculiar interference colours and pores within the shell microstructure (see
419 Maritan et al., 2007). Archaeological features similar to those observed at Jebel Qara have
420 been recently described at the micro-scale by Balbo et al. (2010) and Zerboni (2011); due to
421 the many analogies with them, we interpreted the shells layers inside the studied rock
422 shelters as intentional accumulations related to human activities. The land snails-bearing
423 layers occurring in the rock shelters of the Jebel Qara have to be interpreted as anthropic
424 accumulation of land shells or *escargotières* (*sensu* Lubell et al., 1976).

425 The lithic assemblages associated to these sites, including laminar debitage,
426 sometimes Fasad points, represent the remains of hunter gathers populations (Charpentier,
427 2008; Charpentier and Crassard, 2013). Nevertheless, the identification of accumulations of
428 land snails at Jebel Qara represents an unprecedented evidence of foraging strategy
429 adopted by the Early Holocene human groups in southern Arabia. The frequentation of the
430 area was made possible thanks to a main climatic shift towards wet conditions, in contrast
431 with the aridity that dominated in the area at the transition between the Late Pleistocene and
432 the Early Holocene. New and wetter environmental conditions promoted the ecological
433 settings suitable to the development of the molluscs fauna of the Jebel Qara, representing
434 another type of food resources for these populations. At present, we have no evidence for
435 any kind of connection between the Early Holocene sites of Jebel Qara and the coastal area,

436 as for example no marine shell has been found in the inland sites. Along the coast, sites of
437 that age are extremely rare, as one single cave site has been discovered so far dated to the
438 Early Holocene: the Natif 2 site at about 100 km to the East (publication in preparation).

439 After this phase, the increasing of the Indian Ocean monsoon system and the
440 northward shift of the ITCZ, which was in charge of the formation of calcareous tufa, made
441 the rock shelters at the southern margin of the Jebel Qara unsuitable for life and
442 consequently they were abandoned. During the phase characterized by the most wet
443 environmental conditions at Jebel Qara (between c. 8000 and 5000 cal yr BP), the
444 occurrence of many shell middens distributed along the coast of central Oman (Biagi and
445 Nisbet, 1992, 2006; Biagi, 1994, 2005, 2013; Berger et al., 2013) suggests that later
446 prehistoric groups shifted from the mountains to coastal Oman. Therein, they exploited the
447 resources rendered available by the formation of the mangroves, which was triggered by the
448 oscillations of the level of the sea, but also enhanced thanks to the input of freshwater from
449 inland due to reinforced by the monsoon rain (Lézine et al., 2002; Berger et al., 2005, 2013).

450

451 **6. Conclusions**

452 The infilling of caves and rock shelters of Jebel Qara gave the opportunity to reconstruct the
453 climate changes occurred in the area in the Early to Middle Holocene and to confirm previous
454 regional studies. Furthermore, the geoarchaeological investigations allowed to discover a
455 peculiar and unprecedented strategy of exploitation of natural resources performed by the
456 Early Holocene hunter gatherers.

457 The stratigraphic record represented in the Jebel Qara rock shelters indicates that in
458 this span of time the climate of the area changed from dry conditions, dominated by northern
459 winds, to a wet climate, which was on the contrary dominated by the southern monsoon
460 system, and back again to progressively drier conditions. Our evidence is substantially in
461 accordance with data from the caves of Oman (Fleitmann et al., 2007), which indicate a
462 northward advance of the latitudinal position of the ITCZ (and increased monsoonal
463 precipitation) in the period 10500-9500 cal yr BP, a part of the beginning of monsoon

464 reinforcement, which possibly started some centuries before, as confirmed for instance by
465 Lézine et al. (2007). We can find a good correlation also with the beginning of the withdrawn
466 of the summer monsoon (and southward migration of the ITCZ), which began since c. 7800
467 cal yr BP and reached its maximum at c. 3500 cal yr BP, in response to the decreasing of
468 solar heating (Hoorn and Cremaschi, 2004; Fleitmann et al., 2007). Also in the case of Jebel
469 Qara, the palaeoenvironmental archive suggests a progressive weakening of the intensity of
470 the Indian monsoon, rather than its abrupt interruption.

471 After the arid climate at the Pleistocene/Holocene transition, from c. 10500 to 9500
472 cal yr BP the climatic conditions became more humid, probably in relation with the shift of the
473 monsoon front in a closer position to the Dhofar coast; ecological conditions in this period
474 were favourable to a large development of land mollusc fauna and the land snails were
475 exploited as a food resource by human groups, which settled the rock shelters opening at the
476 wadi bottom. After that, since c. 9000 cal yr BP the enhanced intensity of the monsoon
477 system led to the formation of calcareous tufa and the cavities of Jebel Qara were
478 abandoned and the later prehistoric groups were attracted by other regions. They possibly
479 moved to the coastal plain of Salalah, but the Neolithic archaeological record indicates
480 intensive occupations along the coast of central Oman; therein they exploited the resources
481 rendered available in the mangroves, whose development was favoured by the inland
482 expansion of the monsoon rains.

483

484 **Acknowledgements**

485 We wish to thank the archaeological authorities of the Sultanate of Oman, especially Dr.
486 Sultan Al-Bakri, director of the Department of Excavations and Archaeological Studies, and
487 Prof. Maurizio Tosi, Ministry of Heritage and Culture, the Salalah MHC branch and its
488 welcoming staff, as well as the French Embassy in Oman. VC wishes to thank the
489 'Consultative Commission for Excavations Abroad' of the Ministry of Foreign Affairs for
490 granting the expedition since 2010. RC wishes to thank the Fondation Fyssen (Paris) for the
491 'Subvention de Recherche 2013' grant that greatly contributed to the sedimentological,

492 speleothems and cave filling analyses, radiocarbon and U/Th dating, as well as logistical
493 expenses on the field. For tremendous help on the field, we wish to thank Ali al-Ma'ashani
494 and Federico Borgi, and the welcoming and helpful people of Jebel Qara.

495

496

497 **References**

- 498 Balbo, A.L., Madella, M., Vila, A., Estévez, J., 2010. Micromorphological perspectives on the
499 stratigraphical excavation of shell middens: A first approximation from the
500 ethnohistorical site Tunel VII, Tierra del Fuego (Argentina). *Journal of Archaeological*
501 *Science* 37, 1252–1259.
- 502 Berger, J.F., Charpentier, V., Crassard, R., Martin, C., Davtian, G., Lopez-Saez, J.A.,
503 2013. The dynamics of mangrove ecosysteme, changes in sea level and the
504 strategies of Neolithic settlements along the coast of Oman (6000-3000 cal. BC).
505 *Journal of Archaeological Science* 40, 3087–3104.
- 506 Berger, J.F., Cleuziou, S., Davtian, G., Cattani, M., Cavulli, F., Charpentier, V., Cremaschi,
507 M., Giraud, J., Marquis, P., Martin, C., Méry, S., Plaziat, J.-C., Saliège, J.-F., 2005.
508 Évolution paléographique du Ja'alan (Oman) à l'Holocène moyen: impact sur
509 l'évolution des paléomilieus littoraux et les stratégies d'adaptation des communautés
510 humaines. *Paléorient* 31(1): 46–63.
- 511 Berger, A., Loutre, M.F., 1991. Insolation values for the climate of the last 10 million years.
512 *Quat. Sci. Rev.* 10, 297–317.
- 513 Biagi, P., 1994. A radiocarbon chronology for the aceramic shell-middens of coastal Oman.
514 *Arabian Archaeology and Epigraphy* 5, 17–31.
- 515 Biagi, P., 2005. The shell-middens of the Arabian Sea and Gulf: maritime connections in the
516 seventh millennium BP? In: Al-Ansary, A.R., et al. (Eds.), *The City in the Arab World:*
517 *Evolution and Development*, 7–16.
- 518 Biagi, P., 2013. The shell middens of Las Bela coast and the Indus delta (Arabian Sea,
519 Pakistan). *Arabian Archaeology and Epigraphy*, 1–6.
- 520 Biagi, P., Nisbet, R., 1992. Environmental history and plant exploitation at the aceramic sites
521 of RH5 and RH6 near the mangrove swamp of Qurum (Muscat e Oman). *Bulletin de*
522 *la Société Botanique Française* 139, 571–578.
- 523 Biagi, P., Nisbet, R., 2006. The prehistoric fisher-gatherers of the western coast of the
524 Arabian Sea: a case of seasonal sedentarization? *World Archaeology* 38, 220–238.

525 Bullock, P., Fedoroff, N., Jongerius, A., Stoops, G., Tursina, T., Babel, U., 1985. Handbook
526 for Soil Thin Section Description. Waine Research Publication, Albrighton, ST, USA.

527 Burns, S.J., Matter, A., Frank, N., Mangini, A., 1998. Speleothem-based paleoclimate record
528 from northern Oman. *Geology* 26, 499–502.

529 Charpentier, V., 2008. Hunter-gatherers of the “empty quarter of the early Holocene” to the
530 last Neolithic societies: chronology of the late prehistory of south-eastern Arabia
531 (8000–3100 BC). *Proceedings of the Seminar for Arabian Studies* 38, 59–82.

532 Charpentier, V., Crassard, R., 2013. Back to Fasad... and the PPNB controversy.
533 Questioning Levantine origin in Arabian Early Holocene projectile points technology.
534 *Arabian Archaeology and Epigraphy* 24(1), 28–36.

535 Coque-Delhuille, B., Gentelle, P., 1998. Aeolian dust and superficial formations in the arid
536 part of Yemen. In: Alsharhan, A.S., Glennie, K.W., Whittle, G.L., Kendall, C. (Eds.),
537 *Quaternary Deserts and Climate Change*. Balkema, Rotterdam, 199–208.

538 Coudé-Gaussen, G., 1991. *Les poussières sahariennes*. John Libbey Eurotext, Rome.

539 Courty, M.A., 2001. Microfacies analysis assisting archaeological stratigraphy. In: Goldberg,
540 P., Holliday, V.T., Ferring, C.R. (Eds.), *Earth Sciences and Archaeology*. Kluwer
541 Academic/Plenum Publishers, New York, pp. 205–39.

542 Crassard, R., 2008. The “Wa’shah method”: an original laminar debitage from Hadramawt,
543 Yemen. *Proceedings of the Seminar for Arabian Studies* 38, 3–14.

544 Crassard, R., 2009. Modalities and characteristics of human occupations in Yemen during
545 the Early/Mid-Holocene. *C. R. Geoscience* 341, 713–725.

546 Cremaschi, M., Negrino, F., 2002. The frankincense road of Sumhuram:
547 Palaeoenvironmental and prehistorical background. In: Avanzini, A., (Ed.), *Khor Rori*
548 *Report 1*. Edizioni Plus, Pisa, 325–363.

549 Cremaschi, M., Negrino F., 2005. Evidence for an Abrupt Climatic Change at 8700 14C yr
550 B.P. in Rockshelters and Caves of Gebel Qara (Dhofar-Oman): Palaeoenvironmental
551 Implications. *Geoarchaeology: An International Journal* 20, 559–579.

552 Cremaschi, M., Perego, A., 2008. Patterns of land use and settlements in the surroundings of
553 Sumhuram. An intensive geo-archaeological survey at Khor Rori: report of field
554 season February 2006. In A. Avanzini ed. A port in Arabia between Rome and the
555 Indian Ocean (3rd c. BC - 5th c. AD) Khor Rori report 2. Erma di Bretschneider, Rome,
556 563–573.

557 Cremaschi, M., Zerboni, A., Spötl, C., Felletti, F., 2010. The calcareous tufa in the Tadrart
558 Acacus Mt. (SW Fezzan, Libya). An early Holocene palaeoclimate archive in the
559 central Sahara. *Palaeogeogr. Palaeoclimatol. Palaeoecol.* 287, 81–94.

560 Cremaschi, M., Zerboni, A., Mercuri, A.M., Olmi, L., Biagetti, S., di Lernia, S., 2014. Takarkori
561 rock shelter (SW Libya): an archive of Holocene climate and environmental changes
562 in the central Sahara. *Quaternary Science Review* 101, 36–60.

563 Drysdale, R.N., Zanchetta, G., Hellstrom, J., Fallick, A.E., Zhao, J., Isola, I., Bruschi, G.,
564 2004. The palaeoclimatic significance of a Middle to late Pleistocene stalagmite from
565 the Alpi Apuane karst, central-western Italy. *Earth Planetary Science Letters* 227,
566 215–229.

567 Drysdale, R.N., Zanchetta, G., Hellstrom, J., Maas, R., Fallick, A.E., Pickett, M., Cartwright,
568 I., Piccini, L., 2006. Late Holocene drought responsible for the collapse of Old World
569 civilizations is recorded in an Italian cave flowstone. *Geology* 34, 101–104.

570 Fleitmann, D., Burns, S.J., Mudelsee, M., Neff, U., Kramers, J., Mangini, A., Matter, A., 2003.
571 Holocene Forcing of the Indian Monsoon Recorded in a Stalagmite from Southern
572 Oman. *Science* 300, 1737–1739.

573 Fleitmann, D., Burns, S.J., Neff, U., Mudelsee, M., Mangini, A., Matter, A., 2004.
574 Palaeoclimatic interpretation of high-resolution oxygen isotope profiles derived from
575 annually laminated speleothems from Southern Oman. *Quaternary Science Reviews*
576 23, 935–945.

577 Fleitmann, D., Burns, S.J., Mangini, A., Mudelsee, M., Kramers, J., Villa, I., Neff, U., Al-
578 Subbary, A.A., Buettner, A., Hippler, D., Matter, A., 2007. Holocene ITCZ and Indian

579 monsoon dynamics recorded in stalagmites from Oman and Yemen (Socotra).
580 Quaternary Science Reviews 26, 170–188.

581 Fleitmann, D., Burns, S.J., Pekala, M., Mangini, A., Al-Subbary, A., Al-Aowah, M., Kramers,
582 J., Matter, A., 2011. Holocene and Pleistocene pluvial periods in Yemen, southern
583 Arabia. Quaternary Science Reviews 30, 783–787.

584 Gasse, F., Van Campo, E., 1994. Abrupt post-glacial climate events in West Asian and North
585 Africa monsoon domains. Earth and Planetary Science Letters 126, 435–456.

586 Gé, T., Courty, M.-A., Matthews, W., Wattez, J., 1993. Sedimentary formation processes of
587 occupation surfaces. In: Goldberg, P., Nash, D.T., Petraglia, M.D., (Eds.), Formation
588 processes in archaeological context. Monographs in World Archaeology 17,
589 Prehistory Press, Madison, WI, 149–163.

590 Goldberg, P., Macphail, R.I., 2006. Practical and Theoretical Geoarchaeology. Blackwell
591 Publishing, Oxford.

592 Hanna, S., Al-Belushi, M. 1996. Introduction to the caves of Oman. Sultan Qaboos
593 University, Ruwi.

594 Hellstrom, J.C., 2003. Rapid and accurate U/Th dating using parallel ion-counting
595 multicollector ICP-MS. Journal of Analytical Atomic Spectrometry 18, 1346–1351.

596 Hellstrom, J.C., 2006. U-Th dating of speleothems with high initial ^{230}Th using
597 stratigraphical constraint. Quaternary Geochronology 1, 289–295.

598 Hilbert, Y.H., 2013. Khamseen rock shelter and the Late Palaeolithic-Neolithic transition in
599 Dhofar. Arabian Archaeology and Epigraphy 24(1), 51–58.

600 Hilbert, Y.H., 2014. Khashabian, a Late Paleolithic industry from Dhofar, Southern Oman.
601 BAR International Series 2601. Archaeopress, Oxford.

602 Hoorn, C., Cremaschi, M., 2004. Late Holocene palaeoenvironmental history of Khawr Rawri
603 and Khawr Al Balid (Dhofar, Sultanate of Oman). Palaeogeography,
604 Palaeoclimatology, Palaeoecology 213, 1–36.

605 Lézine, A.M., Saliège, J.-F., Mathieu, R., Tagliatela, T.L., Méry, S., Charpentier, V., Cleuziou,
606 S., 2002. Mangroves of Oman during the late Holocene: climatic implications and
607 impact on human settlements. *Vegetation History and Archaeobotany* 11, 221–232.

608 Lézine, A., Saliège, J., Robert, C., Wertz, F., Inizan, M., 1998. Holocene lakes from Ramlat
609 as-Sab'atayn (Yemen) illustrate the impact of monsoon activity in southern Arabia.
610 *Quaternary Research* 50, 290–299.

611 Lézine, A., Tiercelin, J.J., Robert, C., Saliège, J.F., Cleuziou, S., Inizan, M.L., Braemer, F.,
612 2007. Centennial to millennial-scale variability of the Indian monsoon during the Early
613 Holocene from a sediment, pollen and isotope record from the desert of Yemen.
614 *Palaeogeography, Palaeoclimatology, Palaeoecology* 243, 235–249.

615 Lubell, D., Hassan, F.A., Gautier, A., Ballais, J.-L., 1976. The Capsian Escargotières.
616 *Science* 191, 910–920.

617 Maritan, L., Mazzoli, C., Freestone, I., 2007. Modelling changes in mollusc shell internal
618 microstructure during firing: implications for temperature estimation in shell-bearing
619 pottery. *Archaeometry* 49, 529–541.

620 McClure, H.A., 1976. Radiocarbon chronology of late Quaternary lakes in the Arabian
621 Desert. *Nature* 263, 755–756.

622 Mickler, P.J., Stern, L.A., Banner, J.L., 2006. Large kinetic isotope effects in modern
623 speleothems. *GSA Bulletin* 118, 65–81.

624 Moeyersons, J., Nyssen, J., Poesen, J., Deckers, J., Haile, M., 2006. Age and backfill/overfill
625 stratigraphy of two tufa dams, Tigray Highlands, Ethiopia: evidence for Late
626 Pleistocene and Holocene wet conditions. *Palaeogeography, Palaeoclimatology,*
627 *Palaeoecology* 230, 165–181.

628 Murphy, C.P., 1986. *Thin Section Preparation of Soils and Sediments*. AB Academic
629 Publishers, Berkhamsted, Herts.

630 Neff, U., Burns, S.J., Mangini, A., Mudelsee, M., Fleitmann, D., Matter, A., 2001. Strong
631 coherence between solar variability and the monsoon in Oman between 9 and 6 kyr
632 ago. *Nature* 411, 290–293.

- 633 Nettleton, W.D., Chadwick, O.A., 1996. Late Quaternary redeposited loess-soil development
634 sequences, South Yemen. *Geoderma* 70, 21–36.
- 635 Parker, A.G., Eckersley, L., Smith, M.M., Goudie, A.S., Stokes, S., Ward, S., White, K.,
636 Hodson, M.J., 2004. Holocene vegetation dynamics in the northeastern Rub' al-Khali
637 desert, Arabian peninsula: a phytolith, pollen and carbon isotope study. *Journal of*
638 *Quaternary Science* 19(7), 665–676.
- 639 Parker, A.G., Wilkinson, T.J., Davies, C., 2006. The early-mid Holocene period in Arabia:
640 some recent evidence from lacustrine sequences in eastern and southwestern
641 Arabia. *Proceedings of the Seminar for Arabian Studies* 36, 243–255.
- 642 Shtober-Zisu, N., Amasha, H., Frumkin, A., in press. Inland notches: Implications for
643 subaerial formation of karstic landforms —An example from the carbonate slopes of
644 Mt. Carmel, Israel. *Geomorphology*. doi: 10.1016/j.geomorph.2014.09.004.
- 645 O'Brien, G.R., Kaufman, D.S., Sharp, W.D., Atudorei, V., Parnell, R.A., Crossey, L.J., 2006.
646 Oxygen isotope composition of annually banded modern and mid-Holocene travertine
647 and evidence of paleomonsoon floods, Grand Canyon, Arizona, USA. *Quaternary*
648 *Research* 65, 366–379.
- 649 Parker, A.G., 2009. Pleistocene Climate Change in Arabia: Developing a Framework for
650 Hominin Dispersal over the Last 350 ka. In: Petraglia, M.D., Rose, J.I., (Eds.), *The*
651 *Evolution of Human Populations in Arabia. Vertebrate Paleobiology and*
652 *Paleoanthropology*, 39, Springer Science+Business Media B.V., 39–49.
- 653 Pietsch, D., Kühn, P., 2009. Soil developmental stages of layered Cambisols and Calcisols
654 on Socotra Island, Yemen. *Soil Science* 174, 292–302.
- 655 Pietsch, D., Kühn, P., Brunner, U., Scholten, T., Hitgen, H., Gerlach, I., 2010. Holocene soils
656 and sediments around Ma'rib Oasis, Yemen. Further Sabaeen treasures? *The*
657 *Holocene* 20, 785–799.
- 658 Pirazzoli, P.A., 1991. *World Atlas of Holocene Sea-level Changes*. Elsevier Oceanography
659 Series, Amsterdam.

660 Platel, J.P., 1992. Geological map of Salalah (sheet NE 40-09), explanatory notes. Sultanate
661 of Oman Ministry of Petroleum and Minerals, Orleans.

662 Platel, J.P., Berthiaux, A., Le Metour, J., Beurier, M., Roger, J. 1992. Geological map of
663 Juzor Al Halaaniyaat (sheet NE 10-10). Directorate General of Minerals, Oman
664 Ministry of Petroleum and Minerals, Muscat.

665 Preusser, F., Radies, D., Matter, A., 2002. A 160 ka record of dune development in Southern
666 Arabia and atmospheric circulation patterns. *Science* 296, 2018–2020.

667 Pye, K., 1987. *Aeolian dust and dust deposits*. Academic, London.

668 Pye, K., 1995. The nature, origin and accumulation of loess. *Quat. Sci. Rev.* 14, 653–667.

669 Regattieri, E., Zanchetta, G., Drysdale, R.N., Isola, I., Hellstrom, J.C., Roncioni, A., 2014. A
670 continuous stable isotopic record from the Penultimate glacial maximum to the Last
671 Interglacial (160 to 121 ka) from Tana Che Urla Cave (Apuan Alps, central Italy).
672 *Quaternary Research* 82, 450–461. <http://dx.doi.org/10.1016/j.yqres.2014.05.005>.

673 Reimer, P.J., Bard, E., Bayliss, A., Beck, J.W., Blackwell, P.G., Bronk Ramsey, C., Buck,
674 C.E., Edwards, R.L., Friedrich, M., Grootes, P.M., Guilderson, T.P., Hafliðason, H.,
675 Hajdas, I., Hatté, C., Heaton, T.J., Hoffman, D.L., Hogg, A.G., Hughen, K.A., Kaiser,
676 K.F., Kromer, B., Manning, S.W., Niu, M., Reimer, R.W., Richards, D.A., Scott, M.,
677 Southon, J.R., Staff, R.A., Turney, C.S.M., van der Plicht, J., 2013. INTCAL13 and
678 MARINE13 radiocarbon age calibration curves 0-50,000 years cal BP. *Radiocarbon*
679 55, 1869–1887.

680 Rogers, T.D., 1980. Meteorological records from the mountain region of Dhofar. The
681 scientific results of the Oman flora and fauna survey 1977 (Dhofar). *Journal of Oman*
682 *Studies, Special Report 2*, 55–58.

683 Sale, J.B., 1980. The environment of the mountain region of the Dhofar. The scientific results
684 of the Oman flora and fauna survey 1977 (Dhofar). *Journal of Oman Studies, Special*
685 *Report 2*, 17–24.

686 Sanlaville, P., 1992. Changements climatiques dans la Péninsule Arabique durant le
687 Pléistocène Supérieur et l'Holocène. *Paléorient* 18, 5–26.

688 Sirocko, F., Sarthein, M., Erlenkeuser, H., Lange, H., Arnold, M., Duplessy, J.-C., 1993.
689 Century-scale events in monsoonal climate over the past 24,000 years. *Nature* 364,
690 322–324.

691 Smith, J.R., Giegengack, R., Schwarcz, H.P., 2004. Constraints on Pleistocene pluvial
692 climates through stable-isotope analysis of fossil-spring tufas and associated
693 gastropods, Kharga Oasis, Egypt. *Palaeogeography, Palaeoclimatology,*
694 *Palaeoecology* 206, 157–175.

695 Stoops, G., 2003. *Guidelines for Analysis and Description of Soil and Regolith Thin Sections.*
696 Soil Science Society of America, Madison, WI.

697 Stoops, G., Marcellino, V., Mees, F., 2010. *Interpretation of Micromorphological Features of*
698 *Soil and Regoliths.* Elsevier, Amsterdam.

699 Uerpmann, H.-P., Uerpmann, M., Kutterer, A., Jasim, S.A., 2009. The Neolithic period in the
700 Central Region of the Emirate of Sharjah (UAE). *Arabian Archaeology and Epigraphy*
701 24(1), 102–108.

702 Wilkinson, T.J., 1997. Holocene environments of the high plateau, Yemen. Recent
703 archaeological investigations. *Geoarchaeology* 12, 833–864.

704 Wright, J.S., 2001. “Desert” loess versus “glacial” loess: Quartz silt formation, source areas
705 and sediment pathways in the formation of loess deposits. *Geomorphology* 36, 231–
706 256.

707 Wright, C.A., 1963. The freshwater gastropod molluscs of Western Aden Protectorate.
708 *Bulletin of the British Museum of Natural History* 10, 254–274.

709 Wright, C.A., Brown, D.S., 1980. The freshwater mollusca of Dhofar. *Journal of Oman*
710 *Studies. Special Report* 2, 97–102.

711 Zarins, J., 2001. *The Land of Incense: Archaeological work in the Governorate of Dhofar,*
712 *Sultanate of Oman, 1990-1995.* Muscat: Sultan Qaboos University Publications.

713 Zarins, J., 2013. Hailat Araka and the South Arabian Neolithic. *Arabian Archaeology and*
714 *Epigraphy* 24(1), 109–117.

715 Zerboni, A., 2011. Micromorphology reveals in situ Mesolithic living floors and archaeological

716 features in multiphase sites in central Sudan. *Geoarchaeology: an international*
717 *journal* 26, 365–391.
718

719 **List of tables**

720 Tab. 1. Results of conventional and AMS-¹⁴C dating; calibrated age results are reported as
721 years BC and BP. Calibration according to IntCal13 curve (Reimer et al., 2013).

722 Tab. 2. Essential micromorphological descriptions of samples representative for the four
723 stratigraphic units composing the infilling of the rock shelters.

724 Tab. 3. Results of U/Th dating on calcareous tufa samples KR1 and KR3. The activity ratios
725 [²³⁰Th/²³⁸U] and [²³⁴U/²³⁸U] have been standardized to the HU-1 secular equilibrium
726 standard. Ages were calculated using decay constants of $9.195 \times 10^{-6} \text{ yr}^{-1}$ (²³⁰Th) and
727 $2.835 \times 10^{-6} \text{ yr}^{-1}$ (²³⁴U), and an assumed initial [²³⁰Th/²³²Th] of 1.5 ± 1.5 except KK215-3B,
728 for which a value of 0.8 has been assumed. Depths are from the sample top, and
729 numbers in brackets are the 95% uncertainties in the last digits given.

730

731 **List of figures**

732 Fig. 1. (A) Location of the study area in Oman. (B) Satellite imagery (Google Earth™)
733 representing the main regions cited in the text; the dashed box indicates the position of
734 Fig. 2.

735 Fig. 2. Geomorphology of the Jebel Qara region (modified from Cremaschi and Negrino,
736 2005); the position of the rockshelters whose Holocene infillings were studied is
737 indicated by labels. The location of the archaeological sites identified in the field work is
738 also shown. Key: 1) pediment of the Nejd Desert and gravely wadi bed; 2) desert loess
739 deposits; 3) deep-cut fluvial net; 4) main Holocene calcareous tufa deposits; 5) slope
740 deposits and Holocene alluvial fans; 6) coastal deposits and marine erosion terrace; 7)
741 main scarps; 8) possible Holocene front of the monsoon rain; 9) rock shelters or caves
742 with shell accumulations (Unit C); 10) rock shelters or caves without shell
743 accumulations; 11) open-air sites (see Cremaschi and Negrino, 2005).

744 Fig. 3. Field pictures of (A) a rock shelter in the Jebel Qara area; note the columnar
745 calcareous tufa sectioning its entrance. (B) The sedimentary infilling of a rock shelter
746 sealed by a thick calcareous tufa. Details of the stratigraphic sequence: (C) the

747 lowermost part of the calcareous tufa sealing the sequence (Unit D); (D) the
748 accumulation of land shells (Unit C); (E) the angular breccia with a loessic matrix (Unit
749 B).

750 Fig. 4. Sketches of the infillings of the rock shelters KR-213 (modified from Cremaschi and
751 Negrino, 2005) and GQ-13/23 in the Jebel Qara; the description of each stratigraphic
752 Unit is in the text. Key: 1) bedrock (limestone); 2) clast-supported breccia (Unit A); 3)
753 matrix-supported breccia and loess (Unit B); 4) organic matter-rich layers; 5)
754 accumulations of land shells/*escargotières* (Unit C); 6) calcareous tufa (Unit D); 7)
755 fragments of charcoal; 8) lithic artefacts.

756 Fig. 5. (A) Recovery during field operations of a Fasad point (indicated by the arrow) in the
757 Unit C of GQ-13/23 site (note that it displays a planar orientation, according to the
758 stratigraphy); (B) the drawing of the same item (by. G. Devilder, CNRS).

759 Fig. 6. Photomicrographs of thin sections of the deposits of rock shelter GQ-13/23. (A) Lower
760 part of Unit B, planar orientation of rock fragments forming a matrix-supported angular
761 breccia (XPL). (B) Unit B, transition between a clast to matrix-supported breccia; note
762 the occurrence of micrite pendants on rock fragments (PPL). (C) Unit B, brown silty fine
763 matrix deeply cemented by calcium carbonate with common quartz grains; the arrows
764 indicated small shell fragments (PPL). (D) Upper Unit B, strong redistribution of calcium
765 carbonate cement forming crystalline pedofeatures and enclosing charcoal fragments
766 (indicated by the arrows; XPL).

767 Fig. 7. Photomicrographs of thin sections of the deposits of rock shelter GQ-13/23. (A) Unit
768 C, deep concentration of mollusc fragments in the *escargotières*; note the clast-
769 supported structure and the presence of evidence of heating (see: Maritan et al., 2007)
770 on several shell fragments (PPL). (B) Unit C, note the strong distribution of micrite on
771 shell fragments and in the micromass (XPL). (C) Unit C, brown matrix between two
772 large shell fragments; note the occurrence of charcoal fragments (c) and a fragment of
773 bone (b) (PPL). (D) Lower part of Unit D, note the transition between the accumulation
774 of land shells and the calcareous tufa (XPL). (E) Concentration of charcoal fragments

775 cemented by micrite at the transition between Unit C and Unit D (PPL). (F) Laminated
776 microstructure with common fenestral voids of the calcareous tufa at the basis of Unit D
777 (PPL).

778 Fig. 8. Isotopic profiles (C and O) of the considered samples of flowstones (KR1 and KR3)
779 and position of U/Th dating results according to flowstones' depth.

780 Fig. 9. The cross plots of $\delta^{18}\text{O}$ versus $\delta^{13}\text{C}$ for each sample (Hendy test); the correlation
781 between C and O values are also reported.

782 Fig. 10. Composite oxygen isotope profiles of flowstones KR1 and KR3 compared with the
783 oxygen curve of the Q5 site (Qunf cave, southern Oman) elaborated by Fleitmann et al.
784 (2003). Changes in Holocene summer insolation (according to Berger and Loutre,
785 1991) are also reported.

Figure

[Click here to download high resolution image](#)

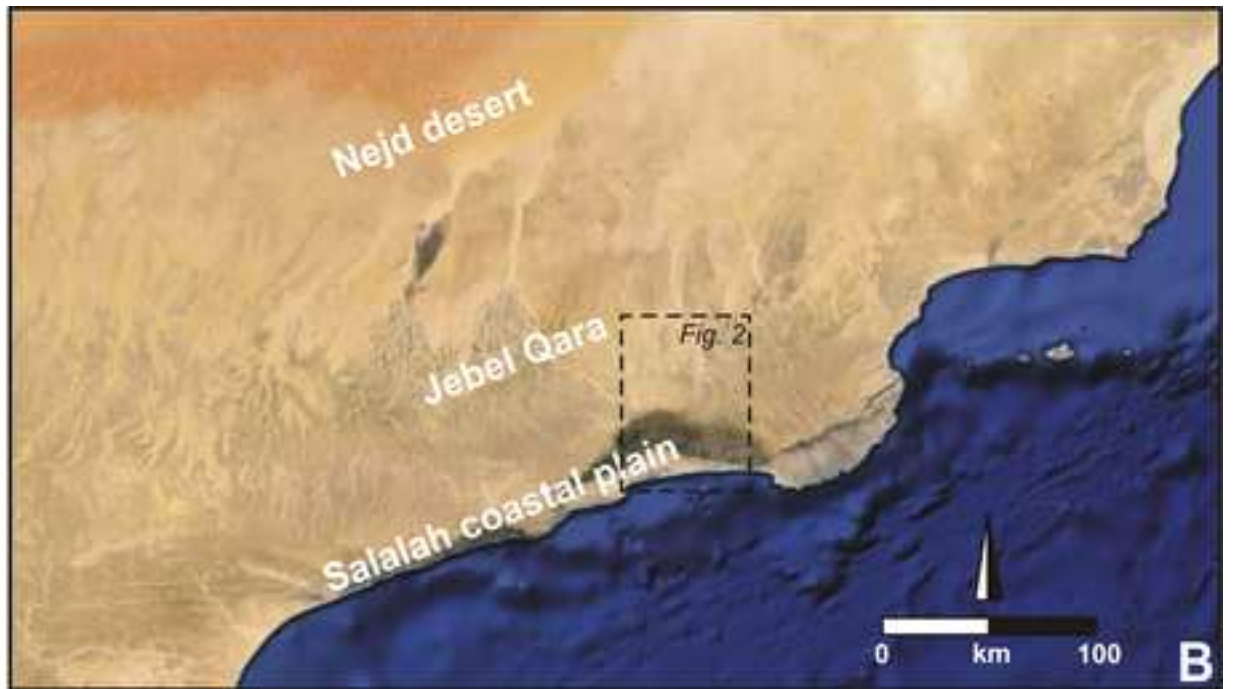
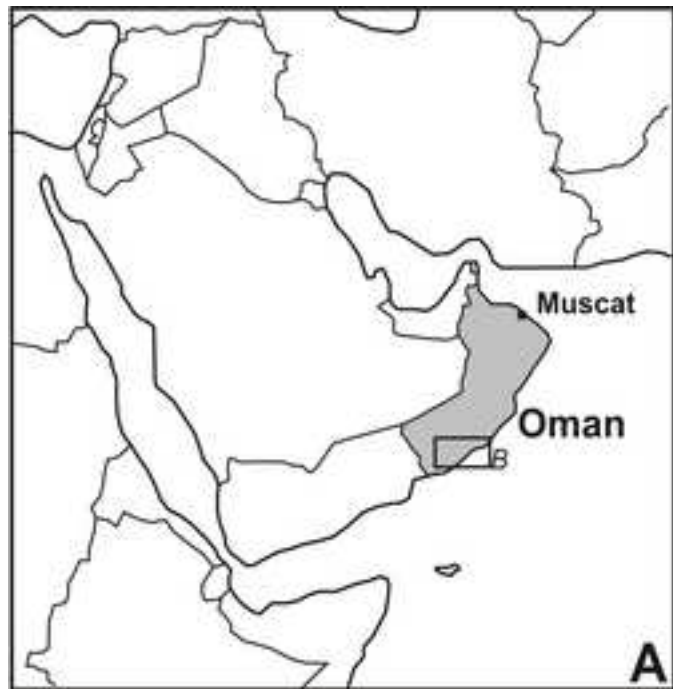


Figure 2
[Click here to download high resolution image](#)

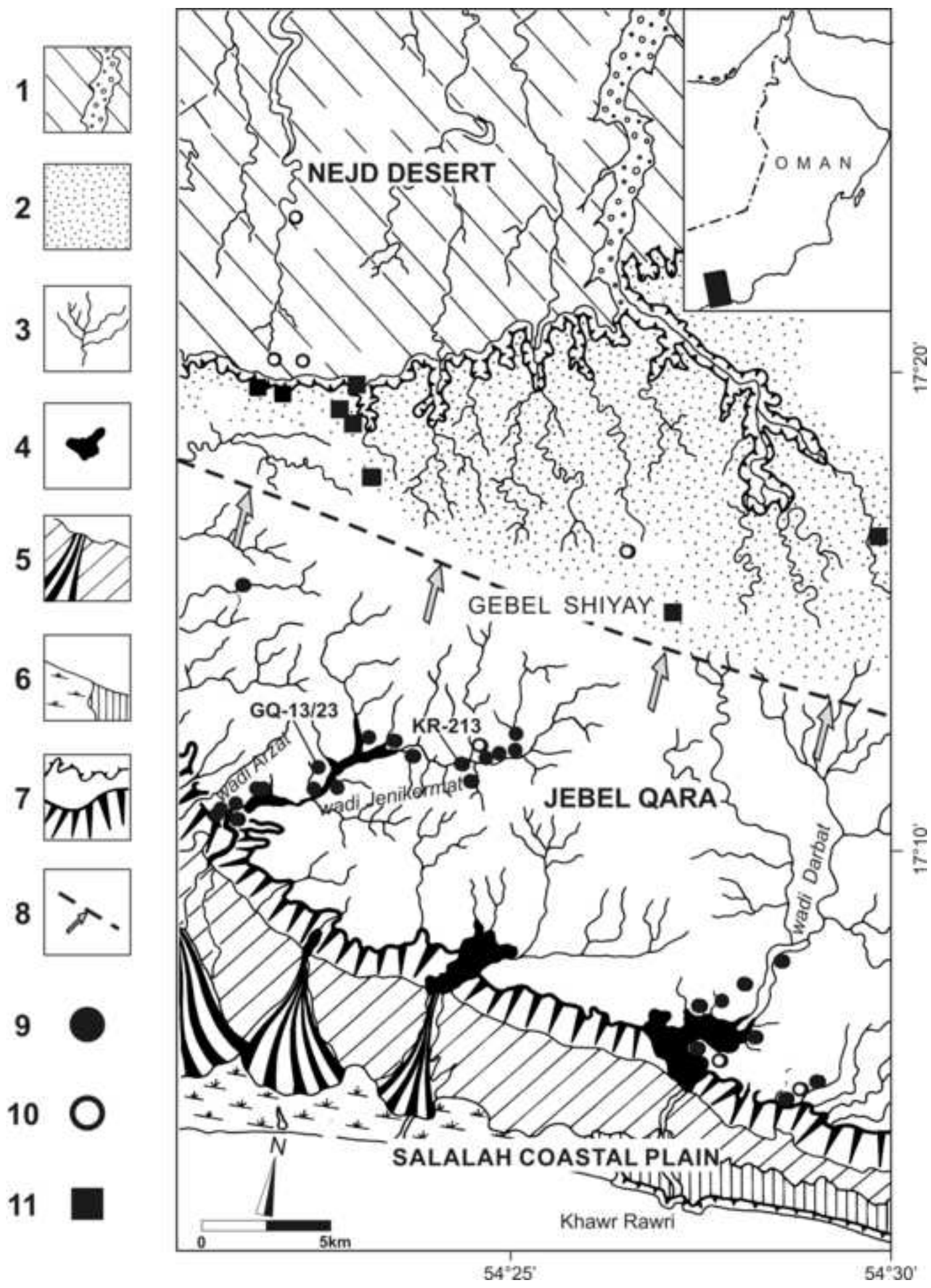


Figure 3
[Click here to download high resolution image](#)



Figure 4
[Click here to download high resolution image](#)

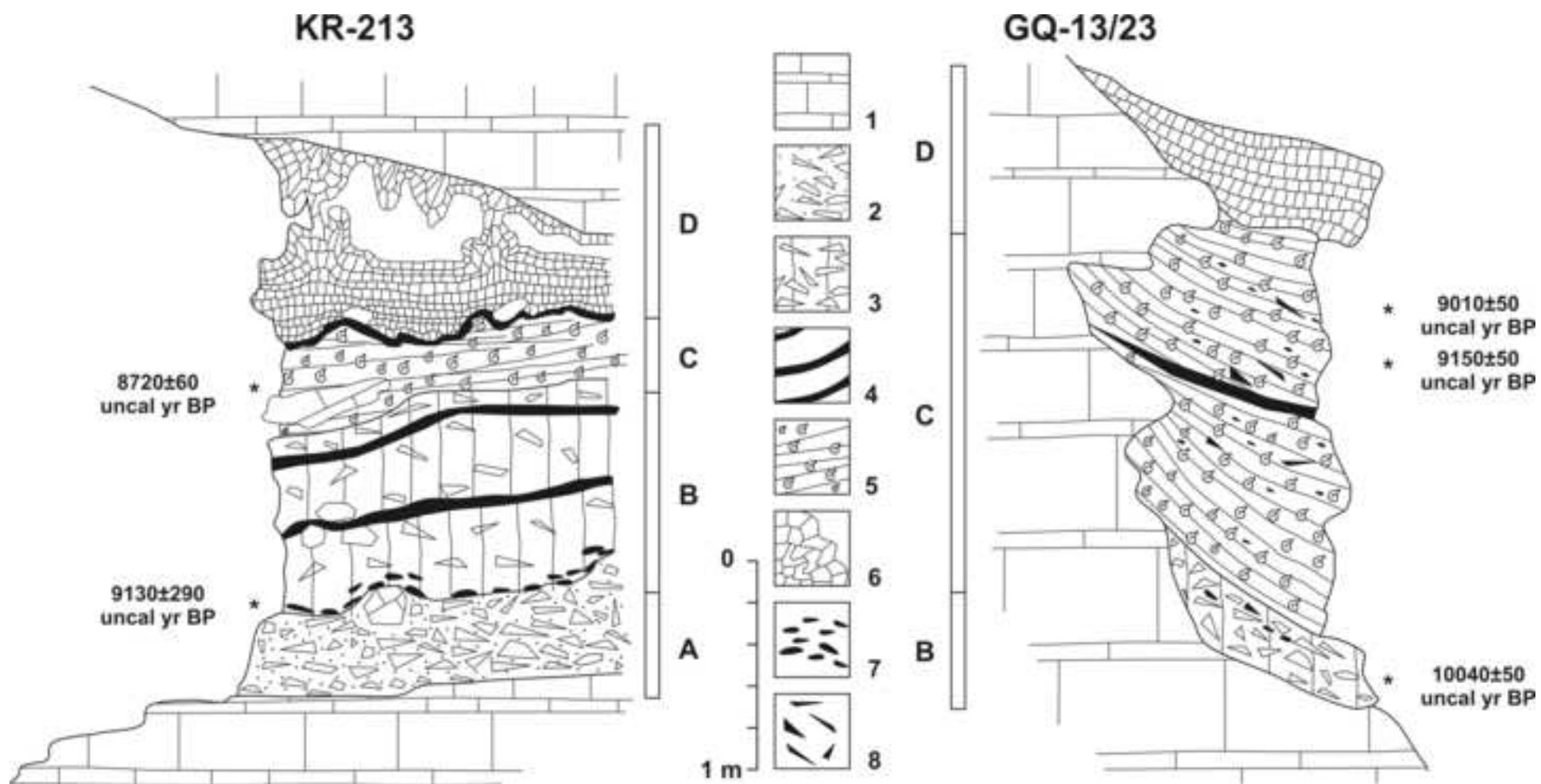


Figure 5
[Click here to download high resolution image](#)

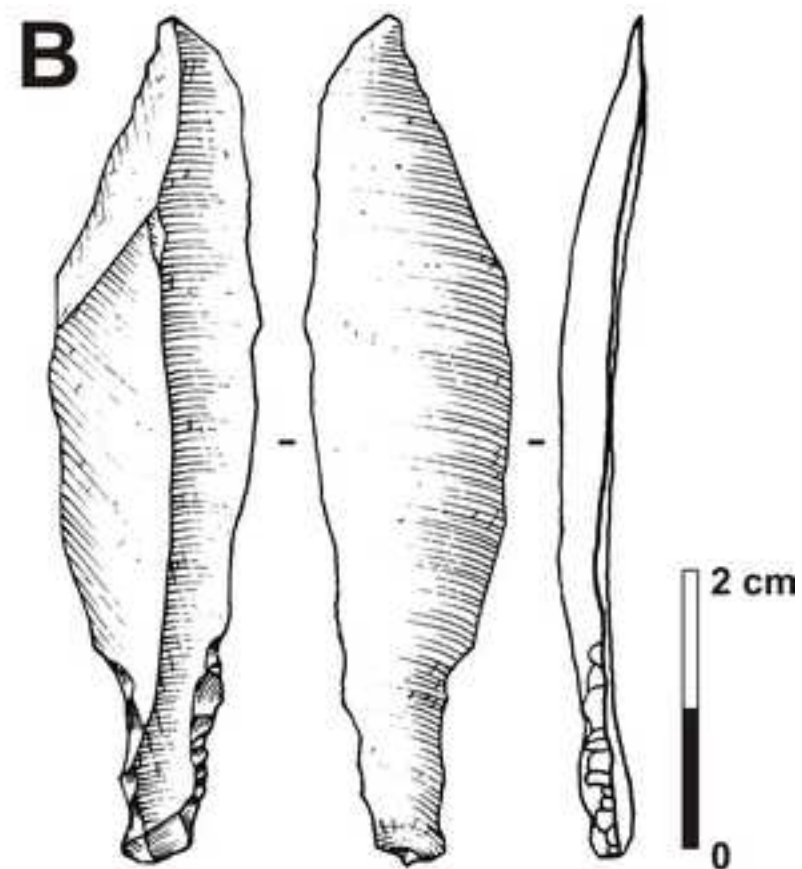


Figure 6
[Click here to download high resolution image](#)

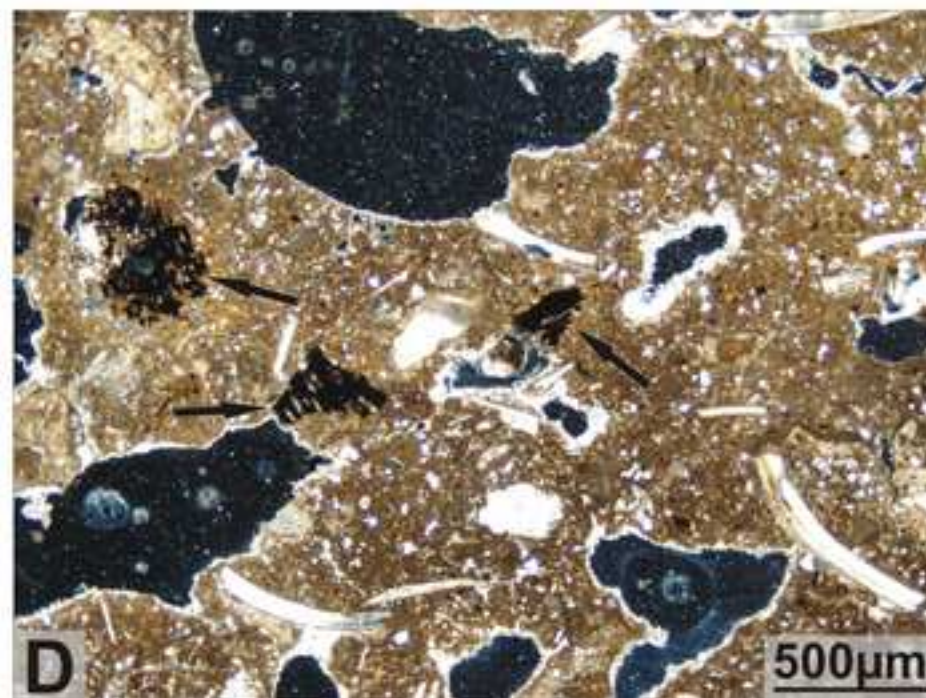
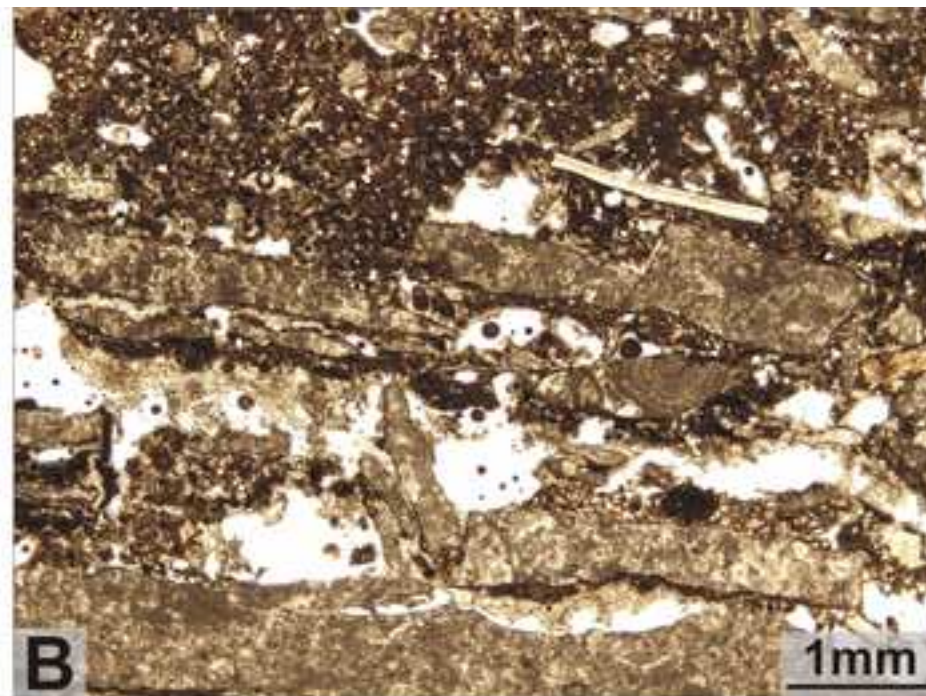
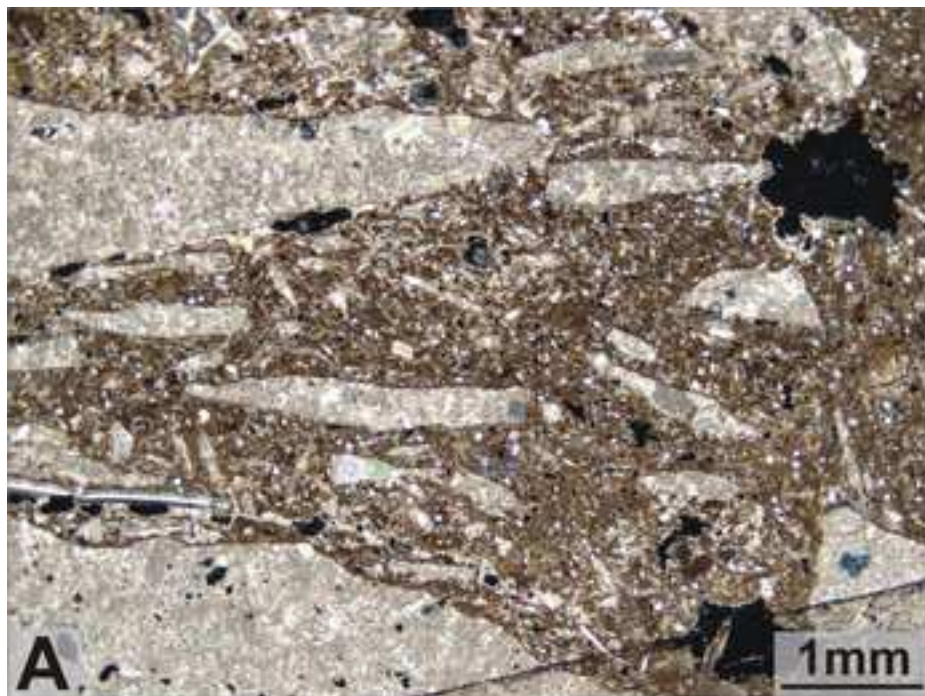


Figure 7
[Click here to download high resolution image](#)

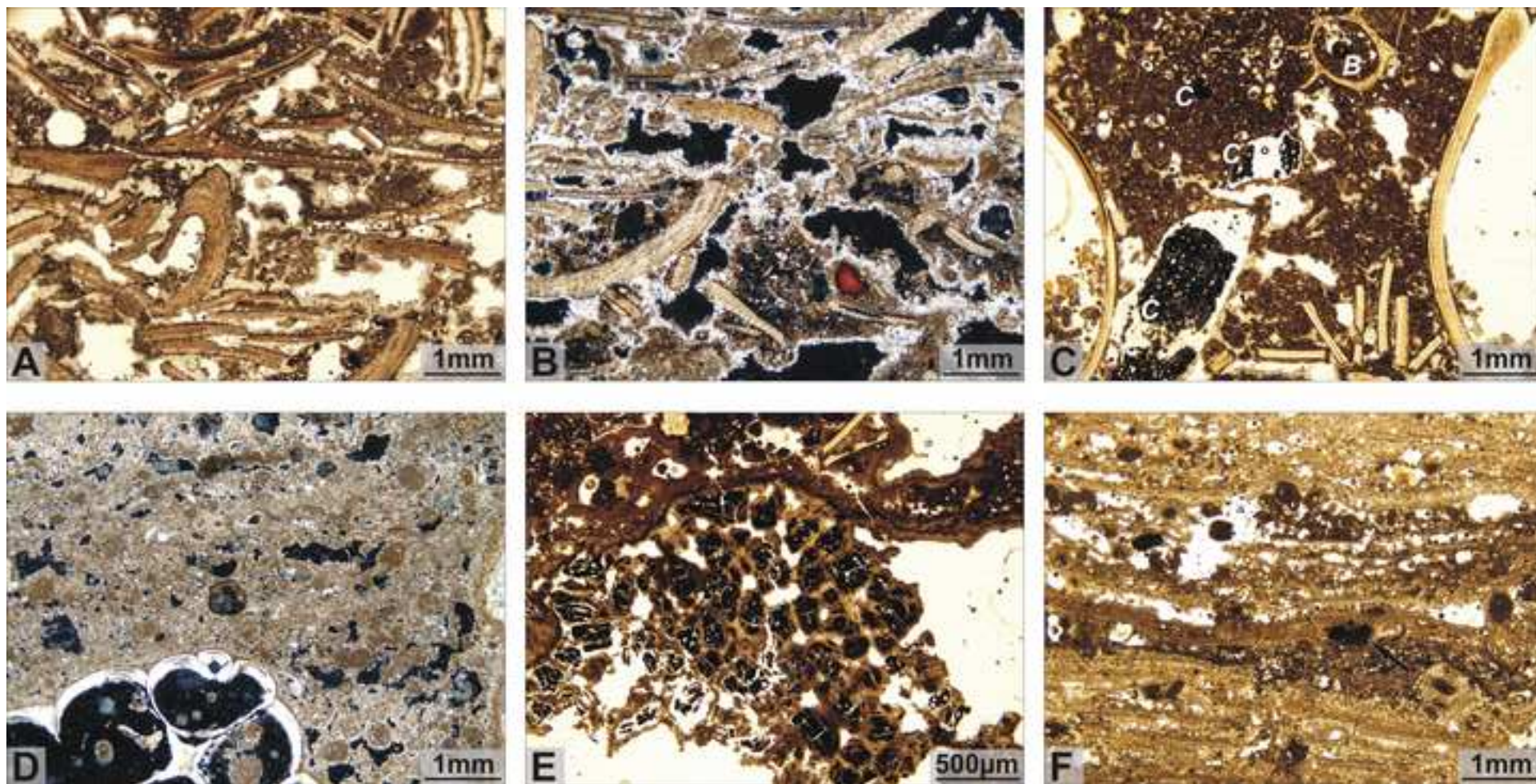


Figure 8
[Click here to download high resolution image](#)

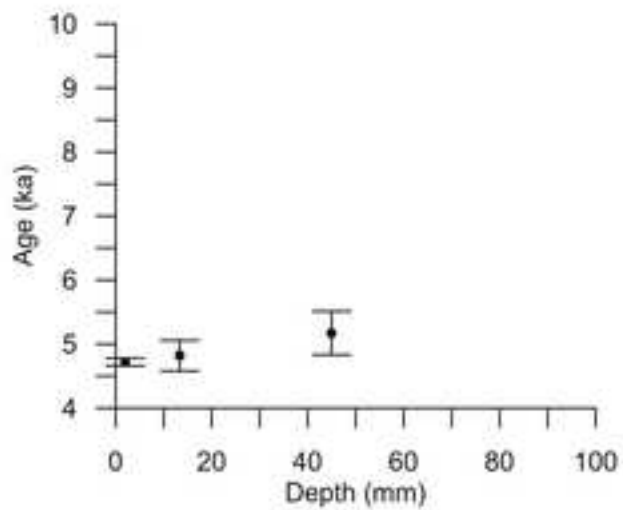
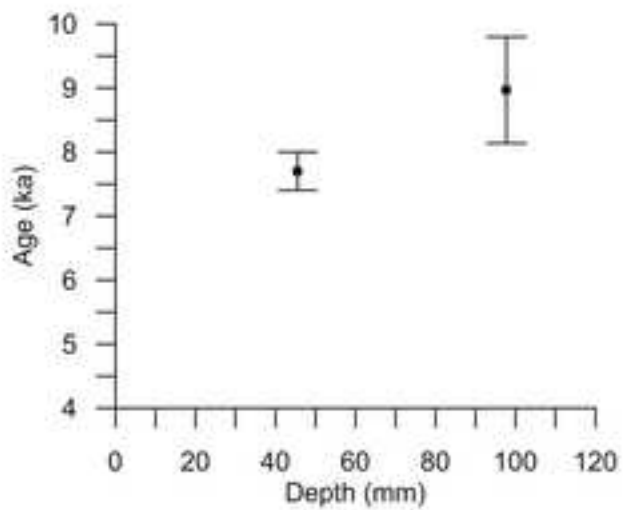
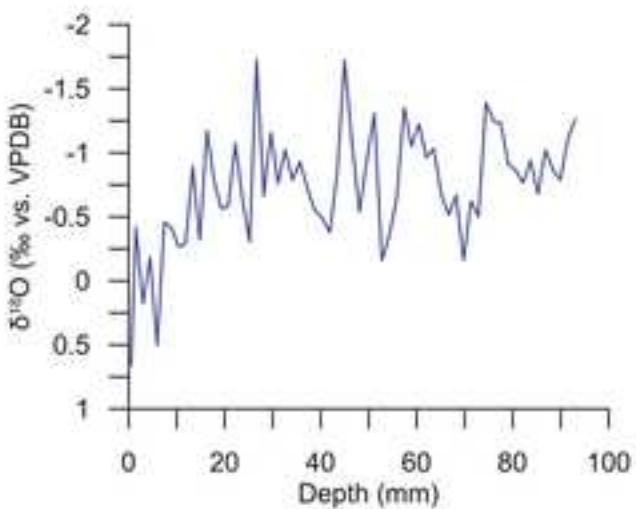
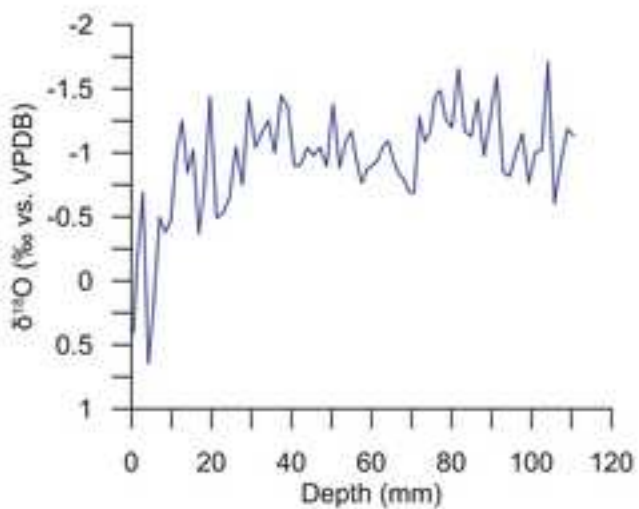
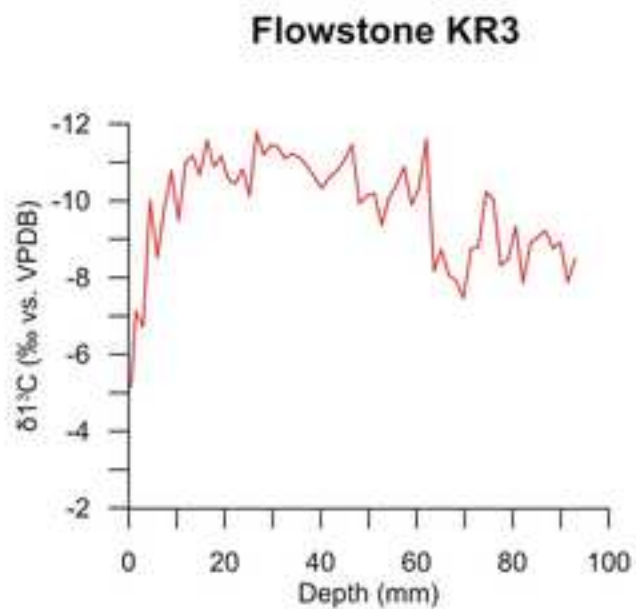
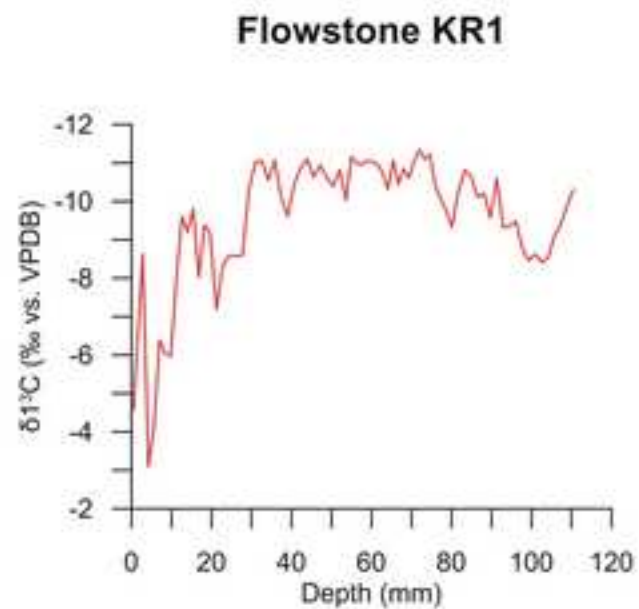


Figure 9

[Click here to download high resolution image](#)

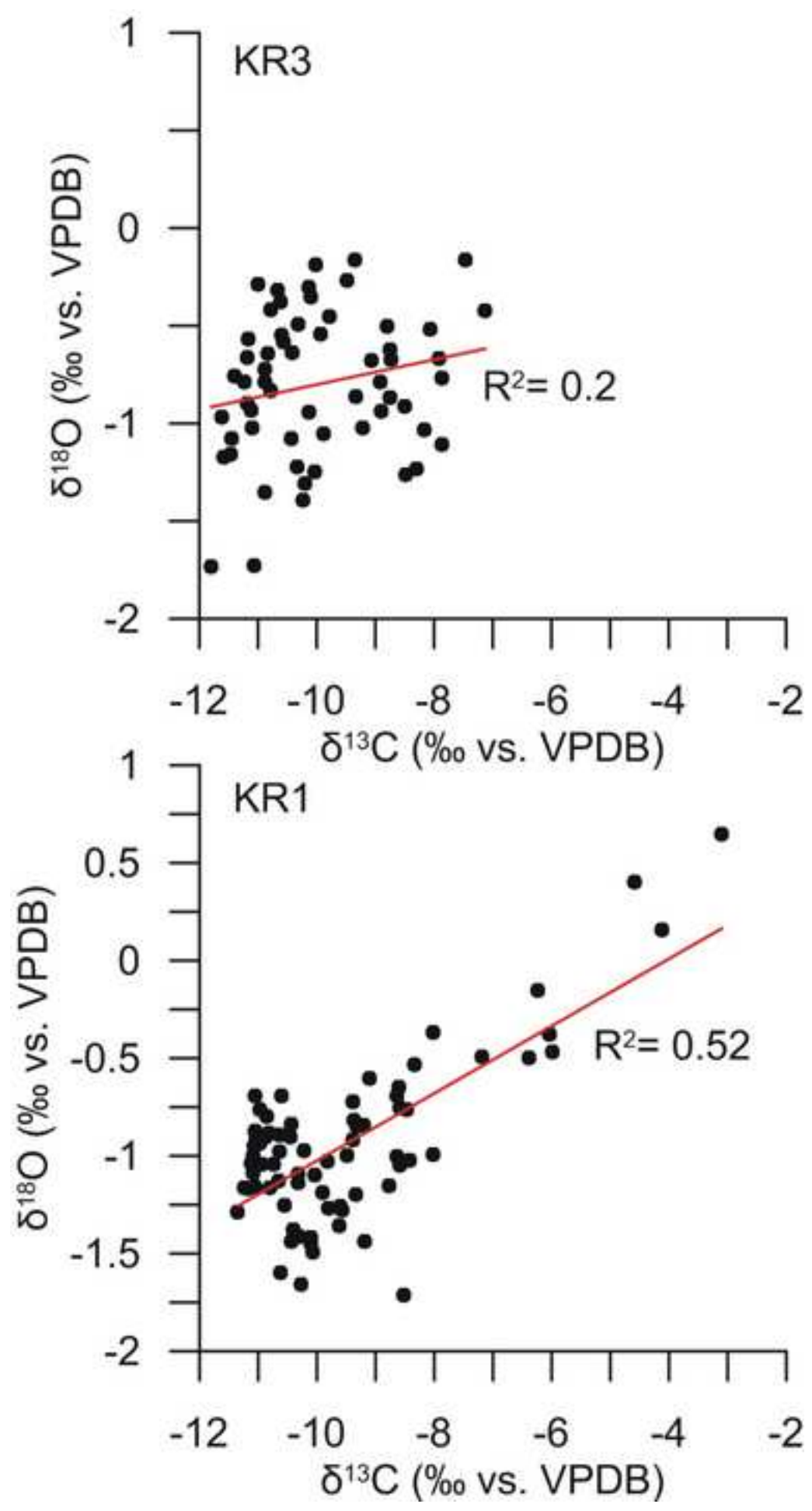


Figure 10
[Click here to download high resolution image](#)

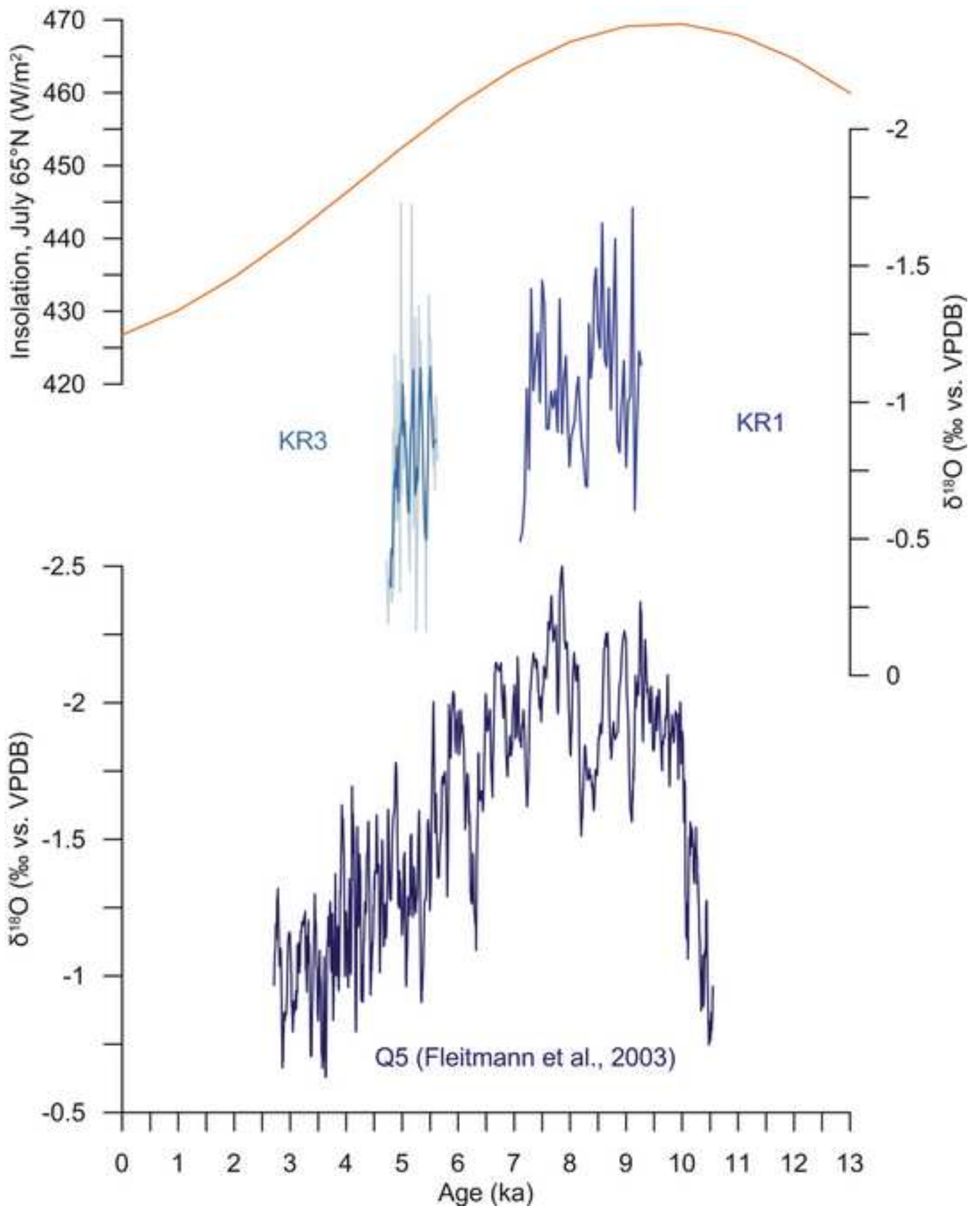


Table 1

Table 1. Results of conventional and AMS-¹⁴C dating; calibrated age results are reported as years BC and BP. Calibration according to IntCal13 curve (Reimer et al., 2013).

Rock shelter	Unit	Lab.-code	AMS- ¹² C age (yr BP)	AMS- ¹² C age cal 2σ	
				(yr cal BC)	(yr cal BP)
GQ-13/ 23	B	Poz-56575	10040±50	9848-9361	11798-11311
GQ-13/ 23	C	Poz-56576	9150±50	8536-8276	10486-10226
KR-213*	B	GX-24065	9130±290	9142-7601	11092-9551
GQ-13/ 23	C	Poz-56574	9010±50	8300-7984	10250-9934
KR-108*	B	GX-23159	8750±50	7965-7603	9915-9553
KR-213*	C	GX-2470-AMS	8720±60	7953-7597	9903-9547

* Radiocarbon dating from Cremaschi and Negrino (2005).

Table 2. Essential micromorphological descriptions of samples representative for the four stratigraphic units composing the infilling of the rock shelters.

Unit	Field interpretation	Mineral constituents	Biogenic constituents	Porosity	Microstructure	b-fabric	c/f related distribution	Pedofeatures
A	Clast-supported angular breccia	Dominant angular fragments of limestone and scarce to common quartz and feldspar grains (sand size) in a silty-clayey micromass	-	Common packing voids and vughs	Intergrain microaggregate	Cristallitic	Gefuric to enaulic	Common micrite coatings on grains and microaggregates, scarce calcite pendent on rock fragments; few calcite nodules; few Fe-nodules; very few clay papulae
B	Matrix-supported angular breccia and loess	Common to scarce angular fragments of limestone, common silt-sized quartz grains and few sand-sized quartz grains in a clay micromass	Few to scarce fragments of shells, few concentrations of angular charcoal fragments; very few, small angular fragments of bone	Common vesicular voids, chambers, and vughs; scarce channels	Spongy to crumb	Cristallitic	Spaced to open porphyric	Common micrite and sparite coatings on voids, scarce calcite pendent on rock fragments; scarce calcite nodules; groundmass impregnated by calcite; few Fe-nodules; very few rounded clay pedorelicts
C	Accumulation of land shells	Scarce quartz and feldspar grains and few subangular fragments of limestone in a silty-clayey matrix	Very abundant to abundant land snails and fragments; scarce to common angular charcoal fragments; few phytoliths; very few weathered vegetal remains; very few fragments of coprolites; shell fragments locally organized in thin horizontal layers with scarce matrix	Common chambers, channels and vughs; locally, packing voids	Crumb to spongy	Cristallitic	Double spaced porphyric; locally, close porphyric	Abundant micrite and sparite coating on crumbs and voids; scarce calcite nodules; groundmass locally impregnated by calcite; few excremental infillings; few Fe-nodules; very few rounded clay pedorelicts
Transition from C to D	Accumulation of land shells to calcareous tufa	Alternating micritic and sparitic layers, including very few fragments of limestone and quartz grains	Common to scarce shell fragments; scarce angular charcoal fragments	Mostly fenestral voids; palnar voids	Laminated	Cristallitic	-	-

Table 3

Table 3. Results of U/Th dating on calcareous tufa samples KR1 and KR3. The activity ratios $^{230}\text{Th}/^{238}\text{U}$ and $^{234}\text{U}/^{238}\text{U}$ have been standardized to the HU-1 secular equilibrium standard. Ages were calculated using decay constants of $9.195 \times 10^{-6} \text{ yr}^{-1}$ (^{230}Th) and $2.835 \times 10^{-6} \text{ yr}^{-1}$ (^{234}U), and an assumed initial $^{230}\text{Th}/^{232}\text{Th}$ of 1.5 ± 1.5 except KR215-3B for which a value of 0.8 has been assumed. Depths are from the stalagmite tip, and numbers in brackets are the 95% uncertainties in the last digits given.

Sample ID	Depth (mm)	^{238}U (ng/g)	$^{234}\text{U}/^{238}\text{U}$ ($\pm 95\%$)	$^{230}\text{Th}/^{238}\text{U} \times 10^3$ ($\pm 95\%$)	$^{234}\text{U}/^{238}\text{U}$ initial ($\pm 95\%$)	Age (ka)	Age corr. (ka)
KR3-B	1	348(1.4)	1.0684(0.0009)	4.78(0.6)	1.0695(0.0009)	4.999(0.064)	4.730(0.06)
KR3-E	13.3	-	1.0637(0.0039)	4.81(0.6)	1.0646(0.0040)	5.029(0.006)	4.820(0.24)
KR3-D	45	-	1.0645(0.0040)	5.25(0.4)	1.0664(0.0041)	5.495(0.046)	5.174(0.34)
KR1-E	45.5	-	1.0788(0.0039)	7.62(0.7)	1.0805(0.0040)	7955(0.075)	7.700(0.30)
KR1-A	97.7	272(20)	1.0820(0.0023)	9.31(0.8)	1.0841(0.0023)	9.770(0.09)	8.990(0.83)